

SUSPENDED MATTER IN MONTEREY BAY,
CALIFORNIA: SOME ASPECTS OF ITS
DISTRIBUTION AND MINERALOGY

Maria Kazanowska

United States Naval Postgraduate School



THESIS

SUSPENDED MATTER IN MONTEREY BAY, CALIFORNIA:
SOME ASPECTS OF ITS DISTRIBUTION AND MINERALOGY

By

Maria Kazanowska

Thesis Advisor

S. P. Tucker

September 1971

Approved for public release; distribution unlimited.

Suspended Matter in Monterey Bay, California:
Some Aspects of its Distribution and Mineralogy

by

Maria Kazanowska
Lieutenant, United States Navy
B.S., Michigan State University, 1966

Submitted in partial fulfillment of the
requirements for the degree of

MASTER OF SCIENCE IN OCEANOGRAPHY

from the

NAVAL POSTGRADUATE SCHOOL
September 1971



ABSTRACT

The distribution of suspended particulate matter in Monterey Bay, California, was characterized by the ratio of light scattering at 45° to that at 135° , by particle volume distributions, and by constituent distributions. X-ray methods were used to identify the mineral constituents. Distributions were highly variable with time and location. Although high scattering ratios and high volume distributions were found in the same vicinity, there appeared to be a lack of correlation between their absolute values. Scattering ratios were found to vary greatly with depth. The minerals detected in the water column at the Pajaro and the Salinas River mouths did not form separate and distinct regions. Of the characteristic minor constituents, jadeite was found to predominate in the Pajaro River area.

TABLE OF CONTENTS

I.	INTRODUCTION	8
II.	COLLECTION AND MEASUREMENT OF SUSPENDED MATTER	11
III.	INTERPRETATION OF DATA	14
IV.	DATA ANALYSES	17
V.	CONCLUSIONS	25
VI.	RECOMMENDATIONS FOR FUTURE STUDY	26
	APPENDIX	74
	REFERENCES	78
	INITIAL DISTRIBUTION LIST	79
	FORM DD 1473	83

LIST OF TABLES

I.	Station Data	66
II.	Pajaro and Salinas River Stream Discharge Data	73

LIST OF FIGURES

1.	Station Locations	27
2.	Scattering Ratio Contours at 2-m Depth	28
3.	Scattering Ratio Contours at 5-m Depth	29
4.	Scattering Ratio Contours at 10-m Depth	30
5.	Volume Contours at 2-m Depth	31
6.	Volume Contours at 5-m Depth	32
7.	Volume Contours at 10-m Depth	33
8.	Transect A Scattering Ratio Contours	34
9.	Transect C Scattering Ratio Contours	35
10.	Transect D Scattering Ratio Contours	36
11.	Transect A Volume Contours	37
12.	Transect C Volume Contours	38
13.	Transect D Volume Contours	39
14.	Transect I Scattering Ratio Contours	40
15.	Transect J Scattering Ratio Contours	41
16.	Transect I Volume Contours	42
17.	Transect J Volume Contours	43
18.	Transect E Scattering Ratio Contours	44
19.	Transect F Scattering Ratio Contours	45
20.	Transect E Volume Contours	46
21.	Transect F Volume Contours	47
22.	Transect G Scattering Ratio Contours	48
23.	Transect G Volume Contours	49
24.	Transect H Scattering Ratio Contours	50

25.	Transect H Volume Contours	51
26.	Montmorillonite Distribution	52
27.	Kaolinite Distribution	53
28.	Muscovite Distribution	54
29.	Illite Distribution	55
30.	Hornblende Distribution	56
31.	Sphene and Hypersthene Distribution	57
32.	Jadeite Distribution	58
33.	Zircon Distribution	59
34.	Serpentine and Apatite Distributions	60
35.	Rutile and Olivine Distributions	61
36.	Epidote Distribution	62
37.	Quartz Distribution	63
38.	Orthoclase Distribution	64
39.	X-ray Intensity Distributions	65

ACKNOWLEDGEMENT

I am deeply indebted to my advisor, Stevens P. Tucker, for providing helpful suggestions and encouragement during the course of this study.

I wish to express by sincere thanks to Prof. Andrews for his interest and help. I also thank Prof. Clark and Prof. Helliwell for their assistance and advice with the X-ray analyses. Finally, the crew of the Naval Postgraduate School boat is to be commended for outstanding performance and endurance.

I. INTRODUCTION

Increasing oceanographic research is being focused on the study of the distribution of suspended particles because they are intimately associated with the physical, chemical, biological, geological, and other processes occurring in the water.

At times the suspended particle distribution has been found to be a more sensitive indicator of water masses than salinity or temperature, for it has been established that concentration occurs at the mixing boundaries of waters of different origin even when differences in other hydrological characteristics are slight [Paramonov, 1965]. The measurement of various parameters in a water mass can be used to trace the particle distribution, which reflects stratification of the waters and provides a basis for characterization [Jerlov, 1959]. Furthermore, the variation in the concentration of suspended material is a sensitive indicator of hydrodynamic conditions and may be used as an indirect method of detecting horizontal currents as well as vertical circulation. Since optical properties of sea water are related to the presence of suspended matter, optical measurements have also been used to characterize water masses.

Direct and indirect methods have been used to determine the content of suspended matter. Direct methods may employ

either filtration or centrifuging to separate the suspended material, which is then dried and weighed. The process is lengthy and involved. A simpler Coulter counter technique may be used to obtain direct particle counts as well as the size fraction distributions. Indirect methods include various optical techniques, all of which involve measuring the scattering or attenuation coefficients of light in water [Jerlov, 1953; Tyler, 1961], and are based on the existence of a linear relationship between the concentration by weight of particles of the same diameter and the scattering or attenuation.

Coastal waters as a rule contain more suspended particles than do deep ocean waters, due to a richer plankton population and larger amounts of both detritus and inorganic matter derived from the land or from the bottom. Rivers carry considerable amounts of sediment into the ocean, and are thus sources of particulate suspended matter close to shore.

Monterey Bay, typical of the semicircular bays common to the California coastline, proveded an advantageous site for studying water mass movement through the investigation of the suspended particulate matter distributions. Prominent headlands at both ends of the bay have created a sheltered conditon over a large portion of it. Studies of the bay's beaches have shown that an essentially static equilibrium has been reached for the present hydrodynamic conditions [Sayles, 1966].

The geology of the area has been extensively investigated, and many detailed reports are available [Martin and Emery, 1967; Wilde, 1965]. The smooth, flat, shelf area of the bay is separated by rugged, steep Monterey Submarine Canyon. Yancy's (1968) investigations have revealed the existence of mineralogical provinces whose development may be ascribed to the major river systems present.

Three rivers draining the adjacent Coast Ranges, an area in excess of 6000 square miles, empty into the bay. Since the rocks of the drainage basins have different mineralogical compositions, the sediment provinces created over the ages within the bay are distinct. The primary source of the inorganic particulate matter entering the bay is the discharge from the principal rivers. More than ninety percent of the runoff occurs in the winter months from December to May.

The aim of this survey was to investigate the water masses in the vicinity of the Salinas and Pajaro Rivers, two sources of particulate matter for Monterey Bay. Previous studies of bottom sediments have shown these two areas to have distinct mineralogical compositions; since the Monterey Canyon separates the regions, no transition zone in the bottom sediment distributions was found. The parameters used in the present work to label water types consisted of an optical index (light scattering), the volume of suspended matter, and X-ray identification of specific inorganic materials found in suspension.

II. COLLECTION AND MEASUREMENT OF SUSPENDED MATTER

To accomplish the aim of this study 52 stations were occupied in the area of interest (Fig. 1). The stations were spaced one-half mile apart and extended up to five nautical miles into the bay. The transects indicated (Fig.1) were used for vertical data analyses. Sampling started in April 1971, when the first nine stations were occupied. In May 1971, three more stations were occupied, and sampling was completed in June 1971. The stations are numbered in the order they were occupied. Since collection of samples in the Salinas river area was spaced over a long time span, these observations tend to be less synoptic than the ones in the Pajaro river area, which was sampled during a comparatively short period.

At each station samples were collected at the surface, in midwater, and near the bottom. A hose was lowered to the appropriate depth, and the samples were pumped up to the surface. Sample containers consisted of 15-gal metal drums lined with polyethylene bags, 5-gal polyethylene bottles, and 125-ml polyethylene bottles. At each of the three depths a 125-ml sample and a 5-gal sample were gathered.

The 125-ml samples were used in the optical and particle distribution analyses. These analyses were carried out within three days of collection. Whenever immediate processing was not possible the samples were stored in the dark at a temperature of about 5 C.

The 5-gal samples were filtered under vacuum using 1.2- μ Millipore filters. The filters were treated with hydrogen peroxide to remove organic material and warm dilute hydrochloric acid to remove carbonates and chlorites if present [Brindley, 1951]. They were then washed with small quantities of distilled water to remove the soluble salts. The washed filters were allowed to air dry. Some were then stored in small plastic petri dishes; others were enclosed in aluminum foil.

A modified Model 4-600 Aminco Light Scattering Microphotometer was used for the optical analysis. The sample was gently agitated and poured into a cylindrical glass cell which was always replaced in the same position in the sample holder. White mercury light was used, and scattering $I(\theta)$ for scattering angles $[\theta]$ of 45° , 90° , and 135° was recorded. Neutral density filters were employed to keep the readings on scale.

The electronic drift of the system was negligible for the few minutes required to make each run. However, when the suspended particles were producing the scattering, there was visual drift over short periods due to sample inhomogeneity. The value for $I(\theta)$ was recorded for approximately one-half minute intervals and average values were used in the analysis of the data.

Particle count and size distributions were determined from the same samples employed in the optical analysis. A Model T Coulter counter with a 254- μ aperture was used. The particle diameters investigated ranged from 3 to 60 μ .

Mineralogical analysis were performed on the dried filters using powder X-ray diffraction techniques. The dried filters were mounted with rubber cement on glass slides and analyzed on a Philips diffractometer. Throughout the analyses $\text{CuK}\alpha$ radiation with a Ni filter was used; the accelerating potential was 35 kv; the beam current was 35 ma; the scanning speed was $1^\circ/\text{min}$; 500 counts/sec represented fullscale; and a 1 sec time constant was employed.

III. INTERPRETATION OF DATA

The scattering of light by suspended material was first treated theoretically in a rigorous way by Mie (1908). Through the application of electromagnetic wave theory a theoretical expression for the light field resulting from the scattering of a plane monochromatic wave by spherical non-absorbing particles was derived. It was established that light scattering depends upon particle size, shape, and relative index of refraction. For low concentrations, and when the scattered light has the same wavelength as incident light, scattering by a system of particles is the sum of the scattered light from individual particles. Thus scattering is directly related to particle concentration.

From the regular behavior of the angular dependence of the volume scattering function Jerlov (1953) showed that an approximate value for the scattering coefficient can be determined from the value of the volume scattering coefficient at 45° . The errors inherent in this process are small. Furthermore, it was also noted that the shape of the angular scattering function for light varies with water type. It is very dissymmetric for turbid water and more symmetric for relatively pure water. The ratio Z , where $Z = I(45^\circ)/I(135^\circ)$, represents the dissymmetry of the angular scattering function about 90° . When Z is large, the curve is very asymmetric, indicating turbid water [Morel, 1965].

Particle size, shape, and composition represent parameters that determine a unique scattering field. Scattering therefore reflects variations in these parameters. The value $I(\theta)$ measured in sea water can be interpreted as a measure of the concentration of particles having a mean diameter.

To supplement the scattering data, particle size distributions were measured with a Coulter counter. The instrument was calibrated with a system of monodispersed $19.0\text{-}\mu$ ragweed pollen. The particle size under investigation ranged from 3 to 60μ in diameter. Since the samples contained particles with a wide range of diameters, the volume of the suspended material within a 2 ml sample was calculated. An attempt was made to correlate Z with volume.

Powder X-ray methods were employed to identify the filter retaining mineral constituents. The Bragg angles of investigation ranged from 5° to 40° . Quantitative analyses could not be conducted; therefore X-ray intensities were not used to indicate constituent concentrations. However, since the sampling techniques and X-ray diffraction methods used were consistent for all of the samples, intensities were used to relate the relative amounts of constituents within the samples. The higher intensities were indicative of greater amounts of constituents present. The analyses fall into four basic categories, "low," "medium," "high," and "background" (Appendix). "Low," "medium," and "high" are self explanatory, while "background" indicates a situation where no signals above the noise background were detected.

The way in which the samples were prepared resulted unavoidably in a tendency toward preferential orientation of the crystals. In a previous study [Yancy, 1968] the mineralogy of the bottom sediments was described. Using this as a guide, known samples of the pure minerals were prepared. The same techniques were used as with the preparations of the collected unknown samples. Thus the d-spacings and the intensities of the various minerals were measured under the same conditions that existed for the unknown constituents. The following criteria were used: montmorillonite was identified from a dominant 13-14 Å peak; kaolinite was identified from peaks at 7 Å and 3.5 Å, the spacing of which was not affected by treatment with warm dilute acid; the mica minerals produced peaks at 10 Å and 3.35 Å (due to the relative abundance of muscovite in the region Yancy concluded that the mica was probably muscovite); sphene had distinctive peaks at 3.2 Å and at 4.7 Å; orthoclase at 3.18 Å and 2.9 Å; zircon at 3.4 Å and at 2.3 Å; quartz at 4.25 Å and 3.3 Å; epidote at 4.2 Å, 4.9 Å and 2.8 Å; jadeite at 3.1 Å, 2.9 Å and 2.7 Å; illite at 4.5 Å, 2.5 Å and 9.9 Å.

IV. DATA ANALYSES

The data used in the analyses are presented in Table 1. The final reduced data were analyzed for horizontal distribution at depths of 2 m, 5 m and 10 m. Vertical distributions are depicted for the transects shown in Fig. 1. Equal value lines were used to assist in localizing areas of high and low values although the contour intervals were not kept strictly constant.

The scattering ration (Z) distribution is contoured for the 2-m, 5-m and the 10-m depths (Figs. 2, 3 and 4). As can be seen, the Z=5 contour remains in the same general position for all depths around the Pajaro River area. The contour for Z=4 does shift with depth. At the 5-m depth the contour is closer to shore than at the 10-m depth. The Salinas River area exhibits a different behavior. The contours tend to parallel the shoreline.

The particle volume contours for 2-m, 5-m and 10-m depths (Figs. 5, 6 and 7) appear to have the same trends as the Z contours in (Figs. 2, 3 and 4). In the Pajaro River region, an increase in volume at 10 m is found. This shows that in that area some bottom influence was exhibited. Overall, much higher volumes are found in the Pajaro River area than in the Salinas River region. This may be due to a plankton bloom, for the volumes decrease substantially with depth. Larger volumes may also be due to a greater influence

of the Pajaro River on the region during the time of investigation, June 1971. As indicated in Table 2, there was a flow from the Pajaro River, while the Salinas River was not contributing particulate matter to the bay at the time of the investigation due to a sand bar across its mouth.

Transects A, B, C and D are perpendicular to the shore in the Salinas River area. Higher Z values were found along transect A (Fig. 8) which is south of the river mouth. Transect C (Fig. 9) indicates that a core of $Z=6$ water has moved in closer to shore. The area enclosed by a $Z=5$ contour has diminished along transect D (Fig. 10), however the proximity to shore remains the same as that in transect C. Particle volume (V) distributions (Figs. 11, 12 and 13) substantiate the Z data, in that the areas of high volume appear in the same general regions as those for high Z.

Transects I and J parallel the shore in the Salinas River area. Transect I (Fig. 14) shows that water with $Z=6$ is upwelled from the Monterey Canyon, toward station 15 from station 19. Water where $Z=5$ is found along the surface dipping down to depth south of the river mouth. Close to the Salinas River mouth at stations 12 and 23 there is also a dip in the $Z=5$ countour. Transect J (Fig. 15) shows the $Z=5$ contour enclosing a core of higher Z values centered around station 22, which is in line with the river mouth. Regions of high and low volumes (Fig. 16) appear in the same locations as high and low Z contours along transect I. However along transect J (Fig. 17) there appears to be a lack of good correlation between the volume and Z distributions.

Transects E and F are perpendicular to the shore in the Pajaro River area. In general, along transect E (Fig. 18) which is off the mouth of the river, higher values of Z are found along the surface and closer to shore. A core of low Z values is found at station 38; the source of the water appears to be offshore. Volume distributions along transect E (Fig. 20) show a core of high values centered around stations 39 and 40, which is not, however, reflected in the scattering ratios (Z). Transect F (Fig. 19), which is farther north, has higher Z values than found along transect E. A core of higher Z values is found at station 32, and this is supported by the volume contour data (Fig. 21). The volume values have been found, in general, to be high along transect E. If a plankton bloom were more pronounced in the area of transect E, then larger particle volumes would be found along with lower scattering ratios. Suspended organic material, in contrast to inorganic material, is normally of a larger size and contributes more to the volume.

Transects G and H are parallel to the shoreline in the Pajaro River area. In transect G (Figs. 22 and 23), which is closer to the shore, an area of relatively low Z and low volume appears to be centered at station 43. This station is in the vicinity of the river mouth. At stations 18 and 17, located at the head of the Monterey Canyon, a region of relatively high Z appears. These observations do not correlate well with the volume observation, for although Z values are much higher than those found at stations to the

north of stations 17 and 18, the volume values are much lower. It must be remembered, however, that stations 17 and 18 were occupied prior to the other stations in the area.

Distributions for Z and volume for transect H (Figs. 24 and 25) once again show two regimes, which are probably attributable to the fact that sampling was not simultaneous but spread out over a period of about two weeks. Stations 20, 19 and 16 were sampled earlier than the other stations. Once again, although Z values were smaller, the volumes were higher during the later sampling period. Station 49, which is near stations 20, 19 and 16, although sampled later, does exhibit characteristics similar to stations in the region. This suggests that a localized plankton bloom occurred in the Pajaro River area.

The extent of variations of the scattering ratio with depth is shown in the Appendix. The largest variation occurred at a depth of about 15 m. This may be due to the fact that at some stations the 15-m depth was closer to the bottom and bottom influences were observed, while in other areas of deeper water 15 m was the mid-water depth.

A plot of scattering ratio as a function of particle volume (Appendix) shows that there is a lack of observed correlation between these parameters. However, as the individual distribution plots did show, there was in general relative correlation between areas of high Z and high volume.

The mineral distribution charts (Figs. 26 to 38) show the stations at which particular minerals were found. The solid lines are drawn to assist in grouping the stations into regions where a given mineral was present in the water column. The cross-hatched areas indicate regions where the specific minerals were found at the 2-m depth.

The uniformity of the clay mineral distributions in the submarine samples as well as their identical character in the Salinas and the Pajaro River samples precluded the use of clay minerals in the mineral province studies [Yancy, 1968]. Of the clay minerals montmorillonite was found at almost all of the stations (Fig. 26). In the top 2 m, the distribution showed a general trend to the south from the Pajaro River area. The area of surface distributions around the Salinas River area was much smaller. Kaolinite is also widely distributed (Fig. 27). Although the surface distributions differ from those for montmorillonite, they tend to be in the same general location. Muscovite was found throughout the Salinas River area (Fig. 28). However, at stations distant from shore in the Pajaro River region muscovite was not detected. The surface distribution is closer to shore in the Pajaro River region, and, in the Salinas River area, muscovite was found at the 2-m depth at all stations. Illite was found in small patches (Fig. 29). The surface distribution is limited primarily to the Salinas River region.

The heavy minerals associated with the Pajaro River and the Salinas River sources have been identified [Yancy, 1968]. Hornblende, augite, and hypersthene were found to be the predominant minerals. The minor constituents were used to distinguish the mineral provinces.

The Salinas River mineralogical province, rich in garnet and hornblende but low in hypersthene, extends south along the shore from the head of the Monterey Canyon and out from shore to a depth of 100 ft. The Pajaro River region is characterized by the minerals restricted to the Franciscan formation (lawsonite, jadeite) and glaucophane. This region, the only source of the Franciscan formation in the bay, can be identified far out in the bay, for the minerals are so distinctive that admixtures from other sources do not make them undetectable.

The heavy mineral distributions found in the present survey are as listed. Hornblende (Fig. 20) was found in the Salinas River area, at the head of the Monterey Canyon, and over a large portion of the Pajaro River area. It was distributed shoreward of the 20-fm contour and tended north in the Salinas River area, while in the Pajaro River region the mineral was found to extend further from shore. At the 2-m depth, hornblende was found over a greater extent of the Pajaro River area than over the Salinas River region. Hypersthene, another of the dominant minerals, was detected at only one station (Fig. 31), while augite and glaucophane were not found at all.

Sphene predominates in the Pajaro River region (Fig. 31), and is found to a smaller extent in the Salinas River area. Jadeite, the characteristic mineral of the Pajaro River area is not restricted to that region alone (Fig. 32). Lawsonite and garnet, the other characteristic minerals, were not detected. Zircon is found in small patches in both areas (Fig. 33). Apatite and serpentine are restricted to the Pajaro River region and to the head of Monterey Canyon (Fig. 34). These two minerals are presented together only because they appear in the same general regions. Once again the following minerals are grouped together for convenience of presentation. Rutile was found at three stations (Fig. 35), while olivine was mainly restricted to the Salinas River region and head of Monterey Canyon. Epidote, common to both regions (Fig. 36), extended over a larger area in the Pajaro River region.

Quartz, the dominant mineral in all of the bottom samples, was found predominantly at stations close to shore (Fig. 37). On the other hand, orthoclase was found more extensively than quartz (Fig. 38). Its surface distribution was close to shore and parallel to the coastline.

The X-ray intensity distribution for the samples analyzed is presented in Fig. 39. In general higher intensities were found close along the shore, close to the river mouths, and at the head of Monterey Canyon. Areas of high intensities are separated by regions of low intensities off both of the river mouths, and at the head of Monterey Canyon. Areas of

high intensities are separated by regions of low intensities off both of the river mouths. These intensity observations are not easily correlated with Z or volume contours, since Z and the particle volume measurements included organic and inorganic materials, while X-ray measurements involved only the inorganic materials.

V. CONCLUSIONS

1. The distribution of suspended materials in Monterey Bay is highly variable, not only with time, but also vertically and horizontally.

2. In general, high scattering ratios and high volume distributions occurred in the same vicinity. However, there appeared to be a lack of correlation between their absolute values.

3. Scattering ratios varied greatly with depth.

4. The minerals detected in the water column did not form separate, distinct regions. Off the Pajaro River the minor constituent, jadeite, was found to predominate.

5. The X-ray intensity distributions showed that areas of high intensities were found close to shore and in the regions of the river mouths.

VI. RECOMMENDATIONS FOR FUTURE STUDY

Since this survey was conducted after the peak outflow period, it is recommended that other measurements be made prior to and during the periods of maximum river outflow. The measurements should be of a quantitative nature so that determinations could be made as to the amount of inorganic suspended materials the rivers contribute to the bay. Also quantitative determinations would allow for establishing relationships among the various parameters used in the water type identification.

The use of an in situ filtration system would enhance the data acquisition process by decreasing sampling time and reducing the possibility of contamination.

Microscopic mineral identification methods in conjunction with X-ray techniques would aid in the identification of even very small quantities of constituents when present.

More stations distributed throughout the bay should be made so that high data density would exist everywhere. This would allow for correlation with other data, such as current measurements as well as salinity and temperature distributions, which are available for the bay. Hydrographic casts should be made at each station at the time that particulate matter data are collected, so that correlations between temperature, salinity, and particle distributions could be established.

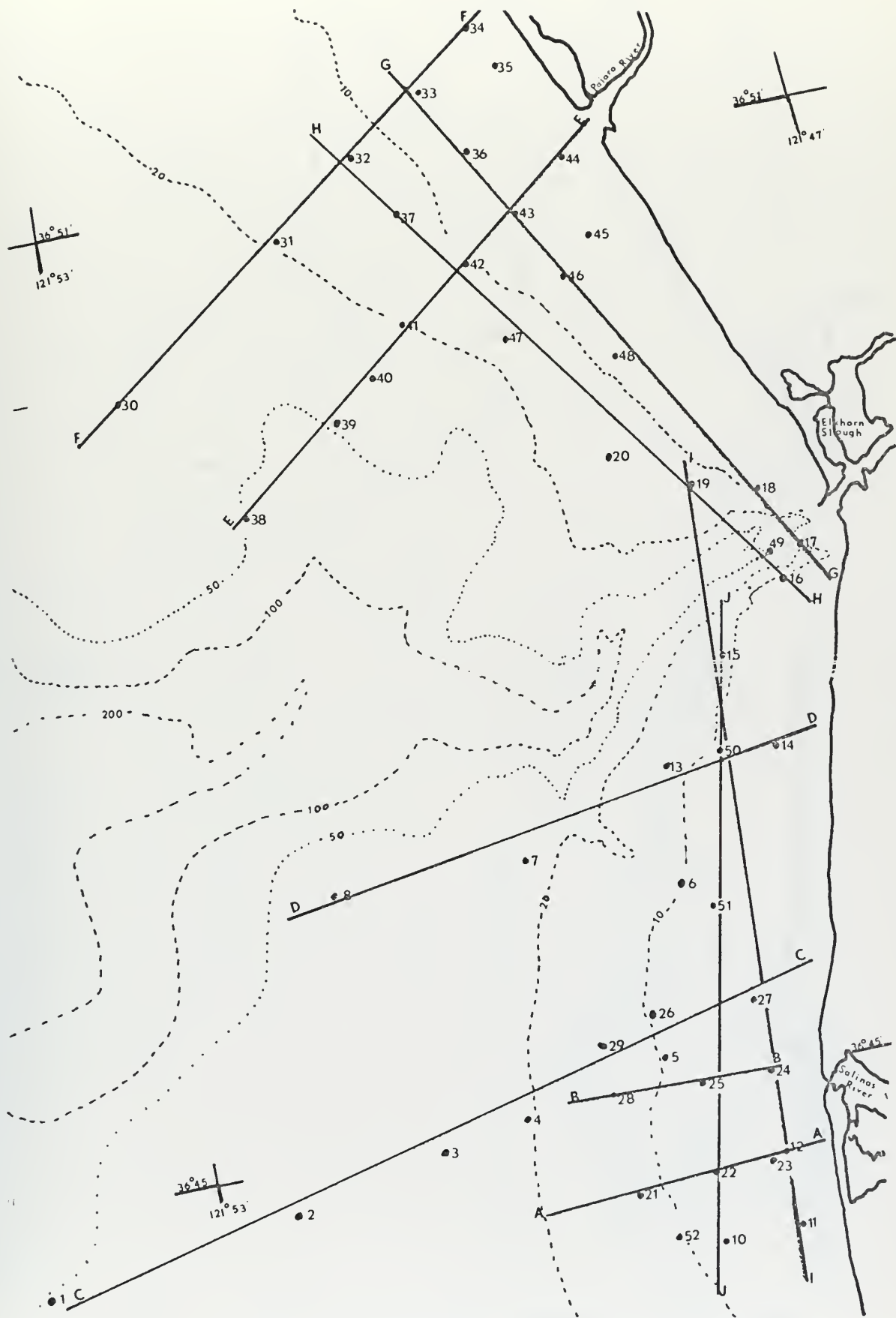


Fig. 1. Station Locations

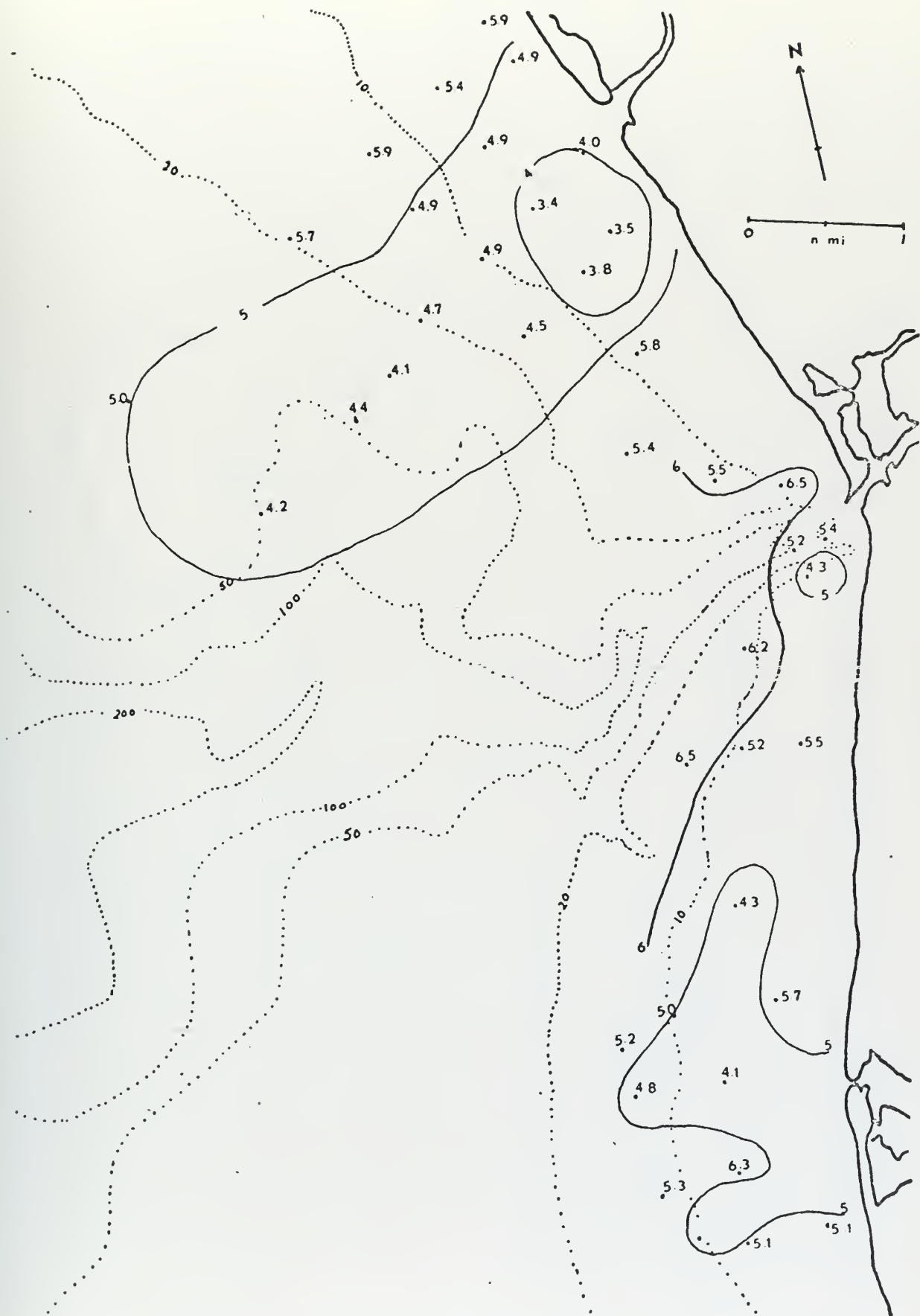


Fig. 3. Scattering ratio contours at 5-m depth

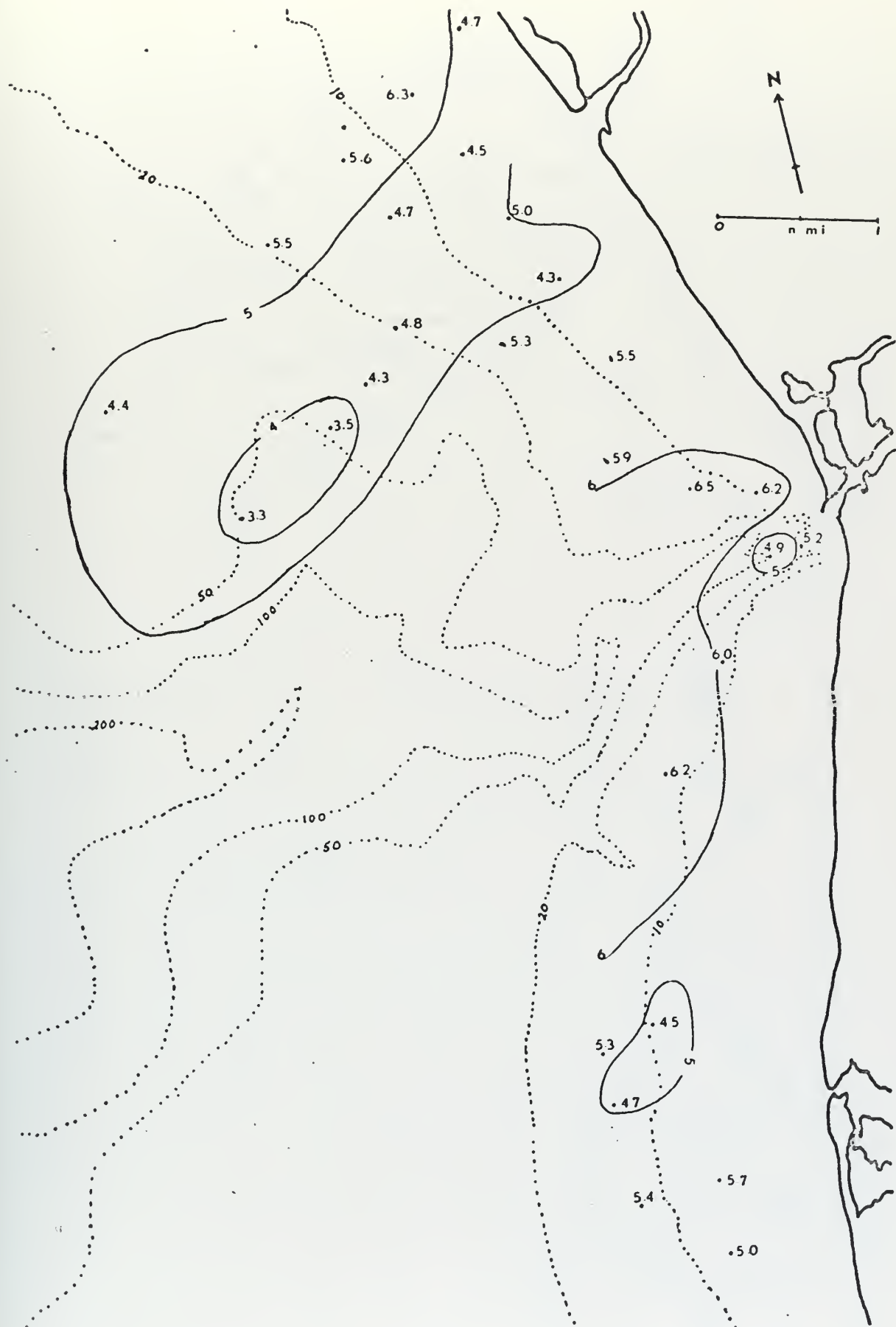


Fig. 4. Scattering ratio contours at 10-m depth

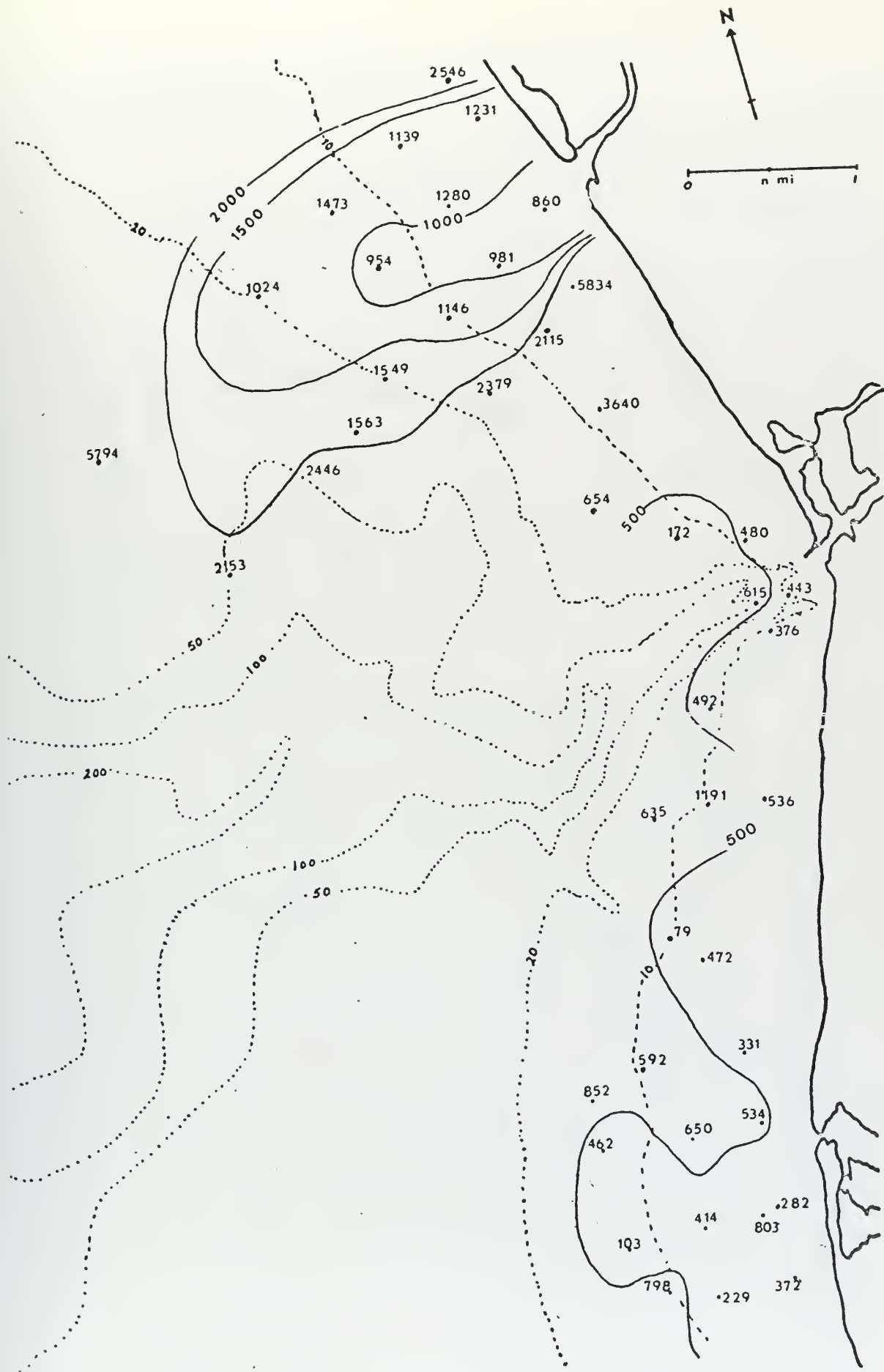


Fig. 5. Volume contours at 2-m depth (Volume $\times 10^{-14} \text{ m}^3$)

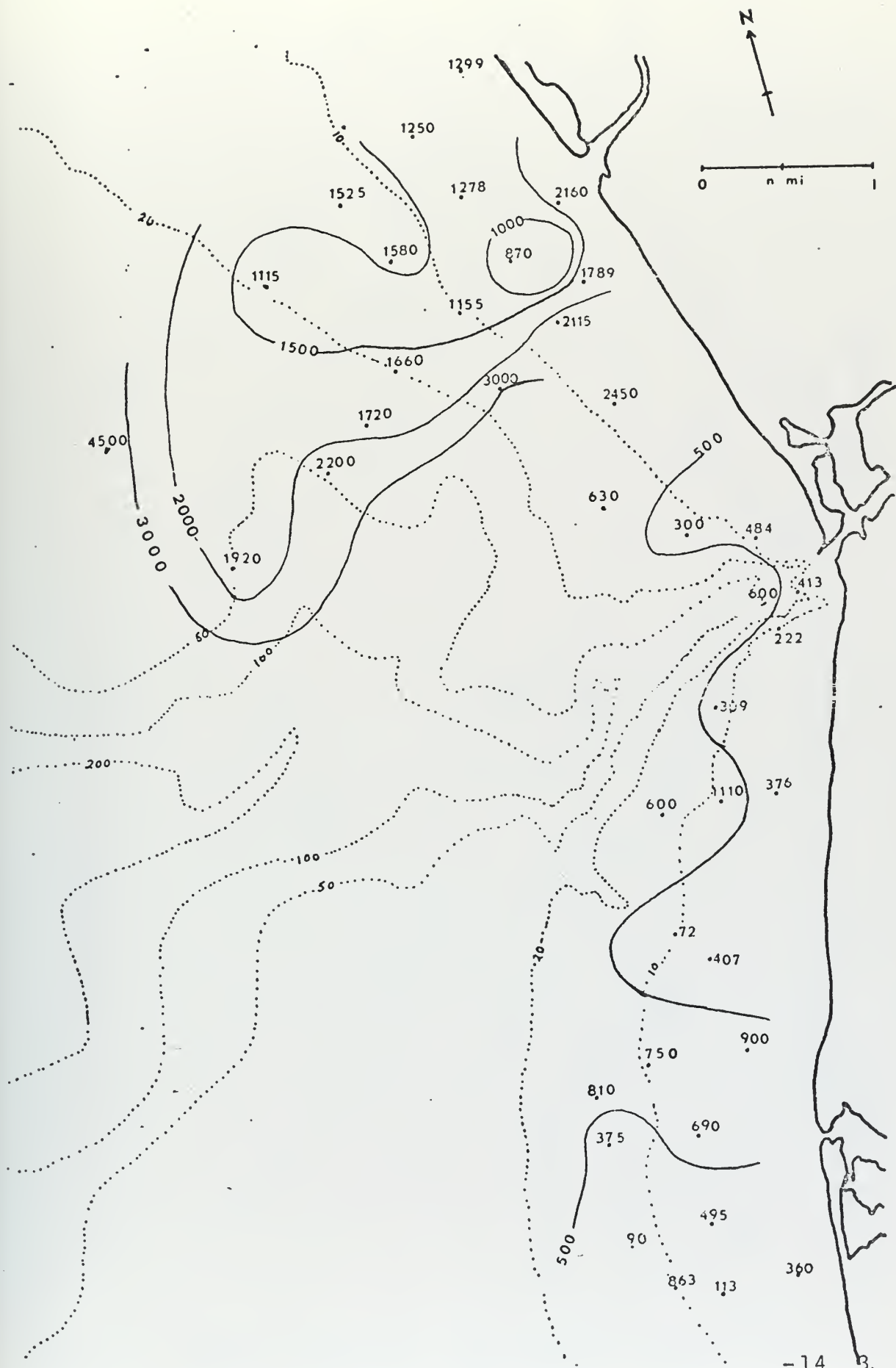


Fig. 6. Volume contours at 5-m depth. (Volume $\times 10^{-14} \text{ m}^3$)

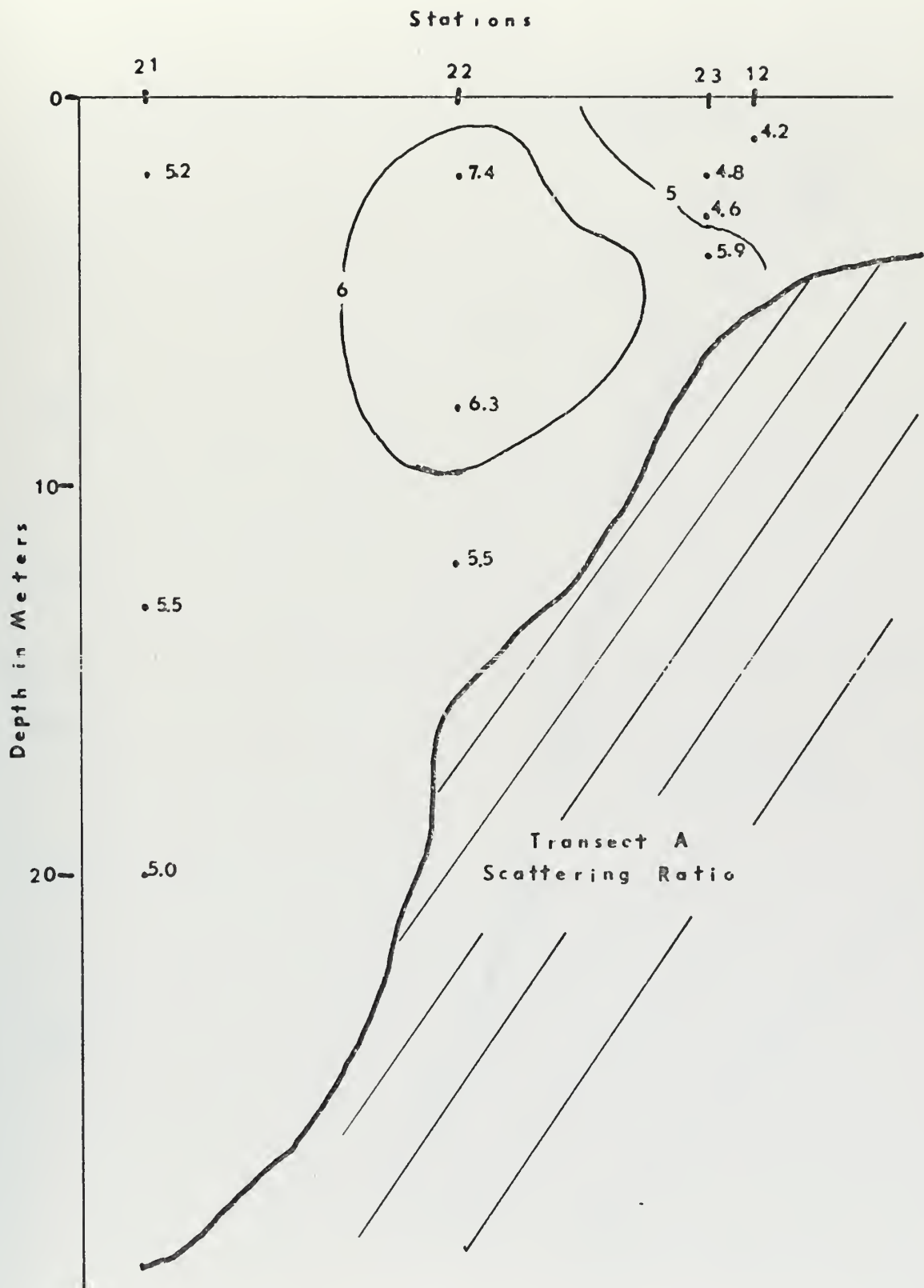


Fig. 8. Transect A Scattering Ratio Contours

Stations

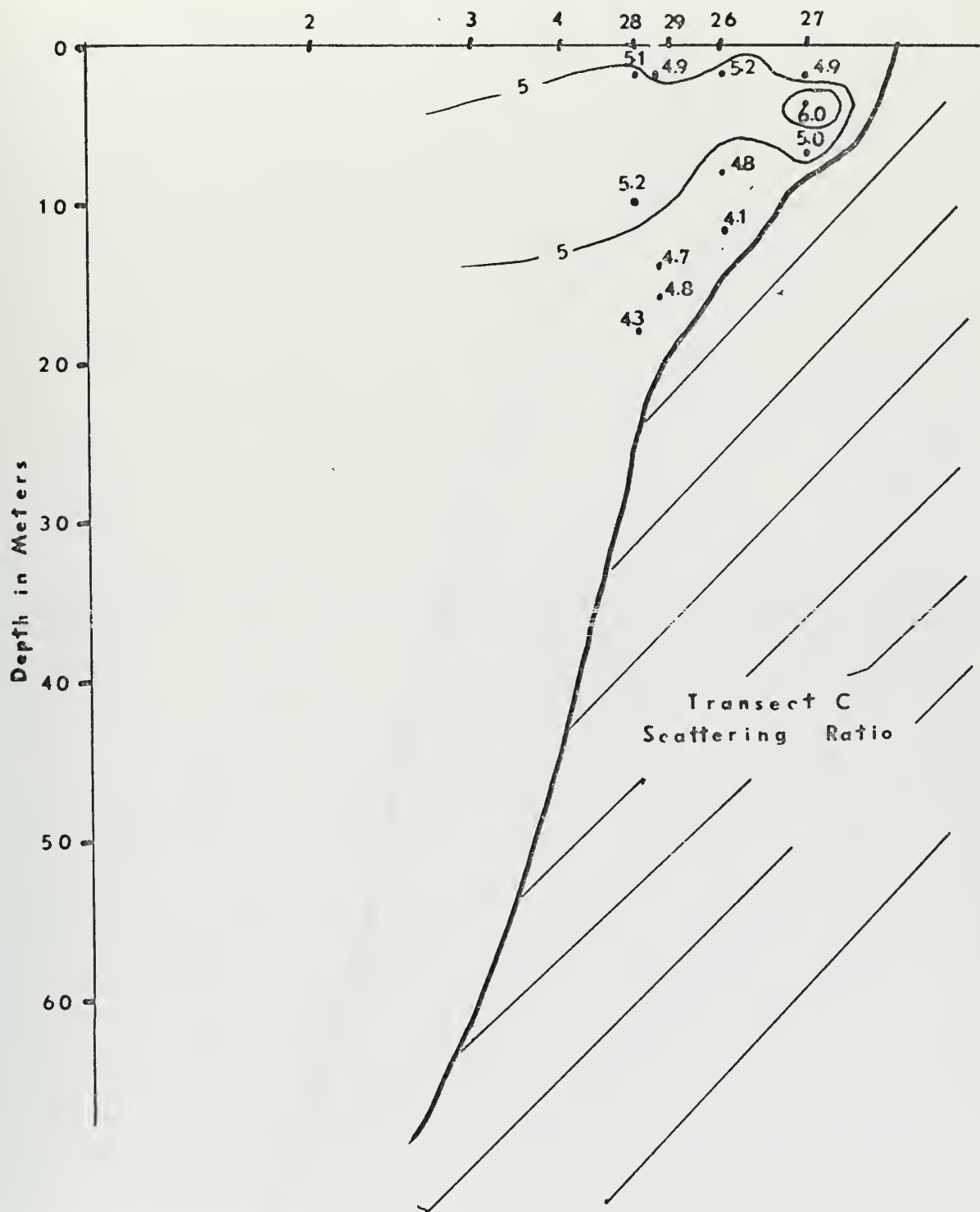


Fig. 9. Transect C Scattering Ratio Contours

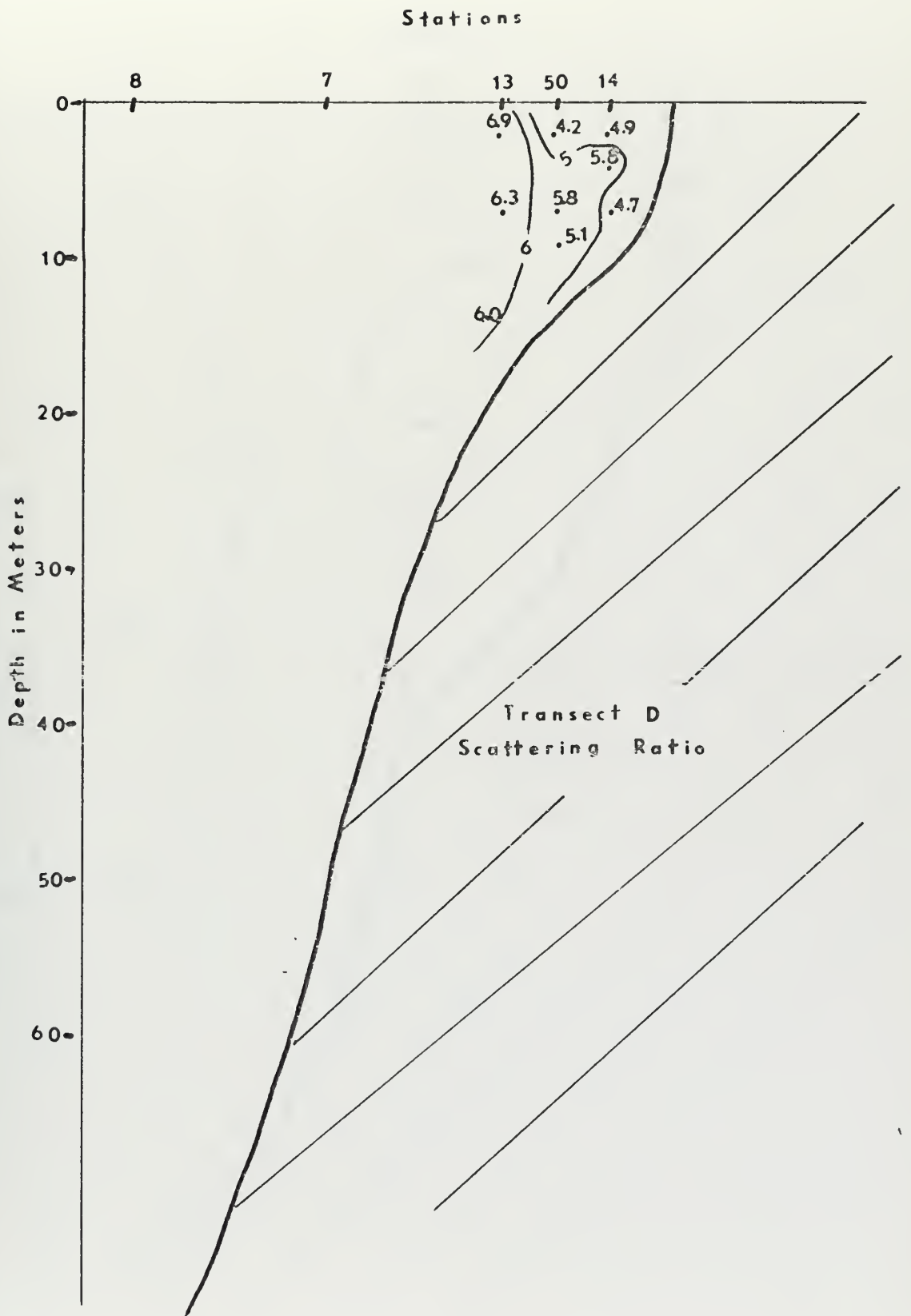


Fig. 10. Transect D Scattering Ratio Contours

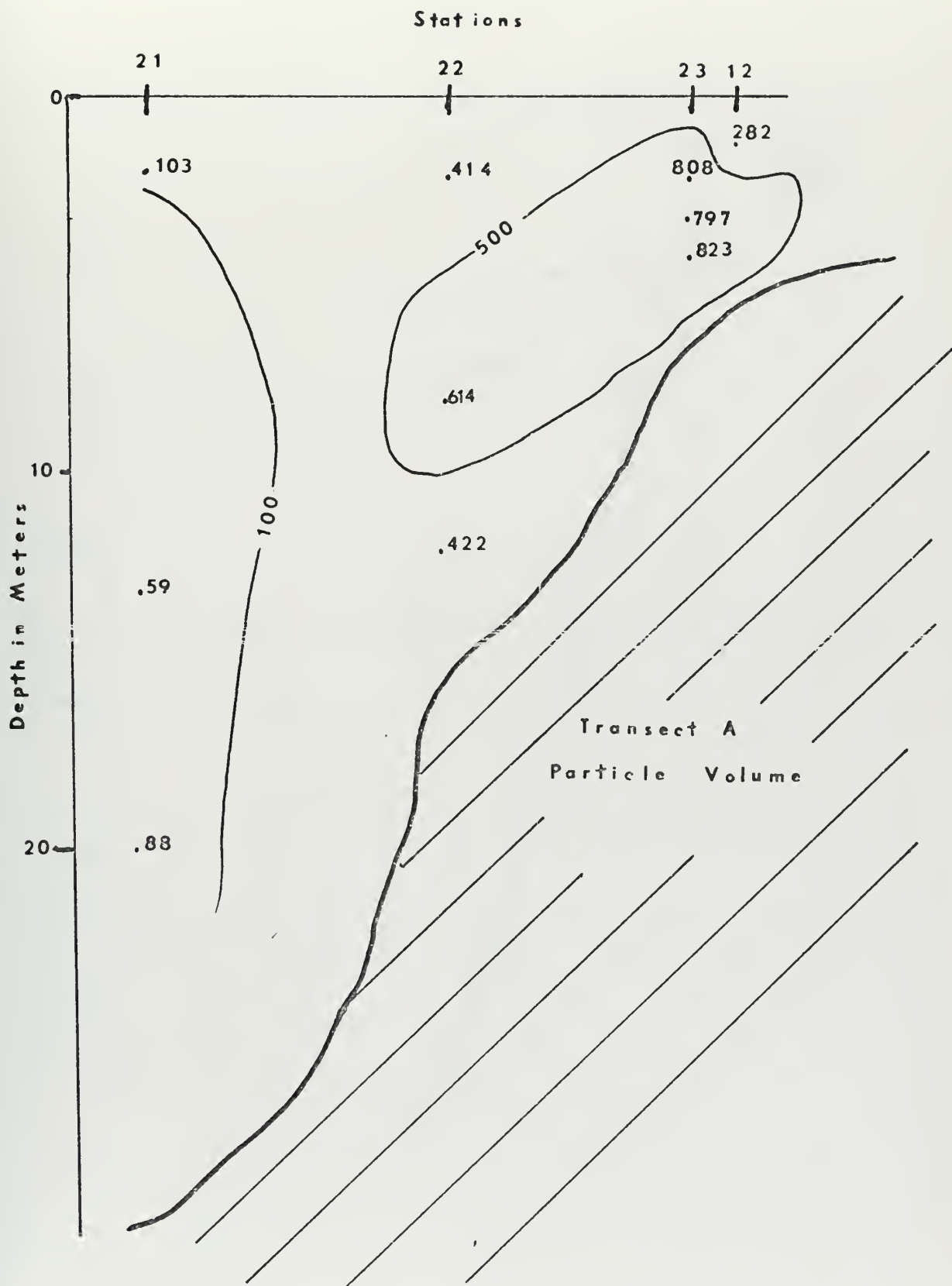


Fig. 11. Transect A Volume Contours

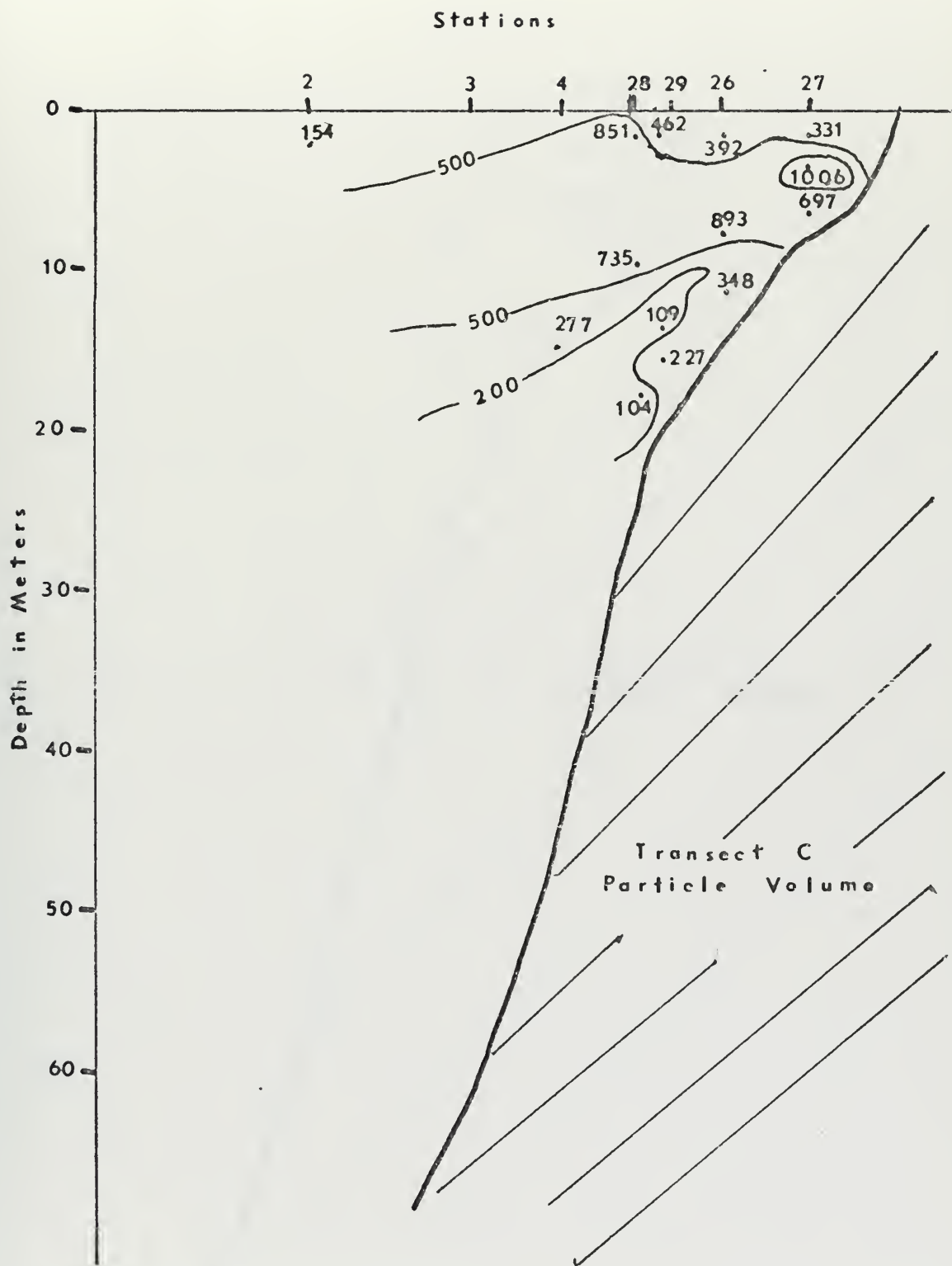


Fig. 12. Transect C Volume Contours

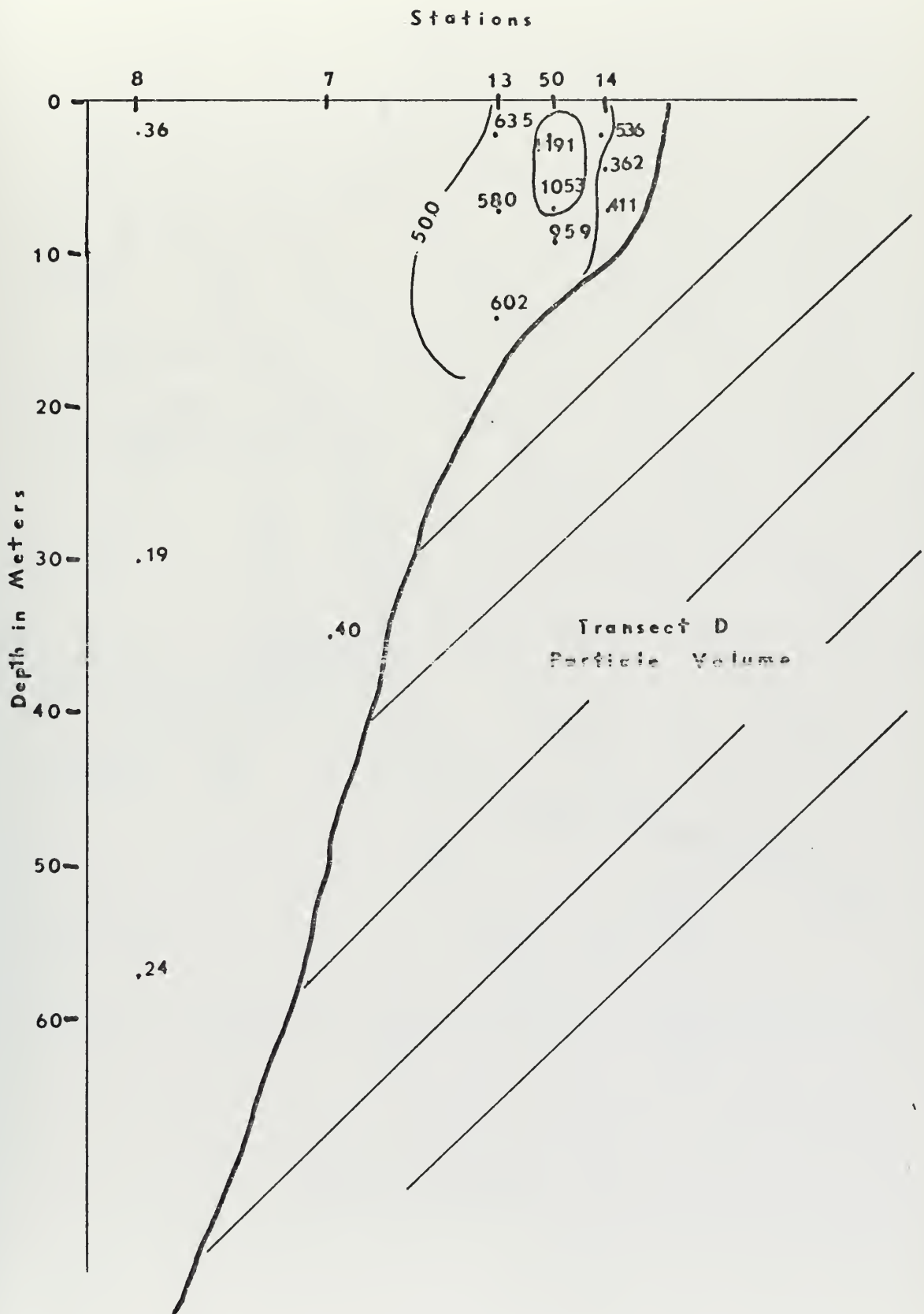


Fig. 13. Transect D Volume Contours

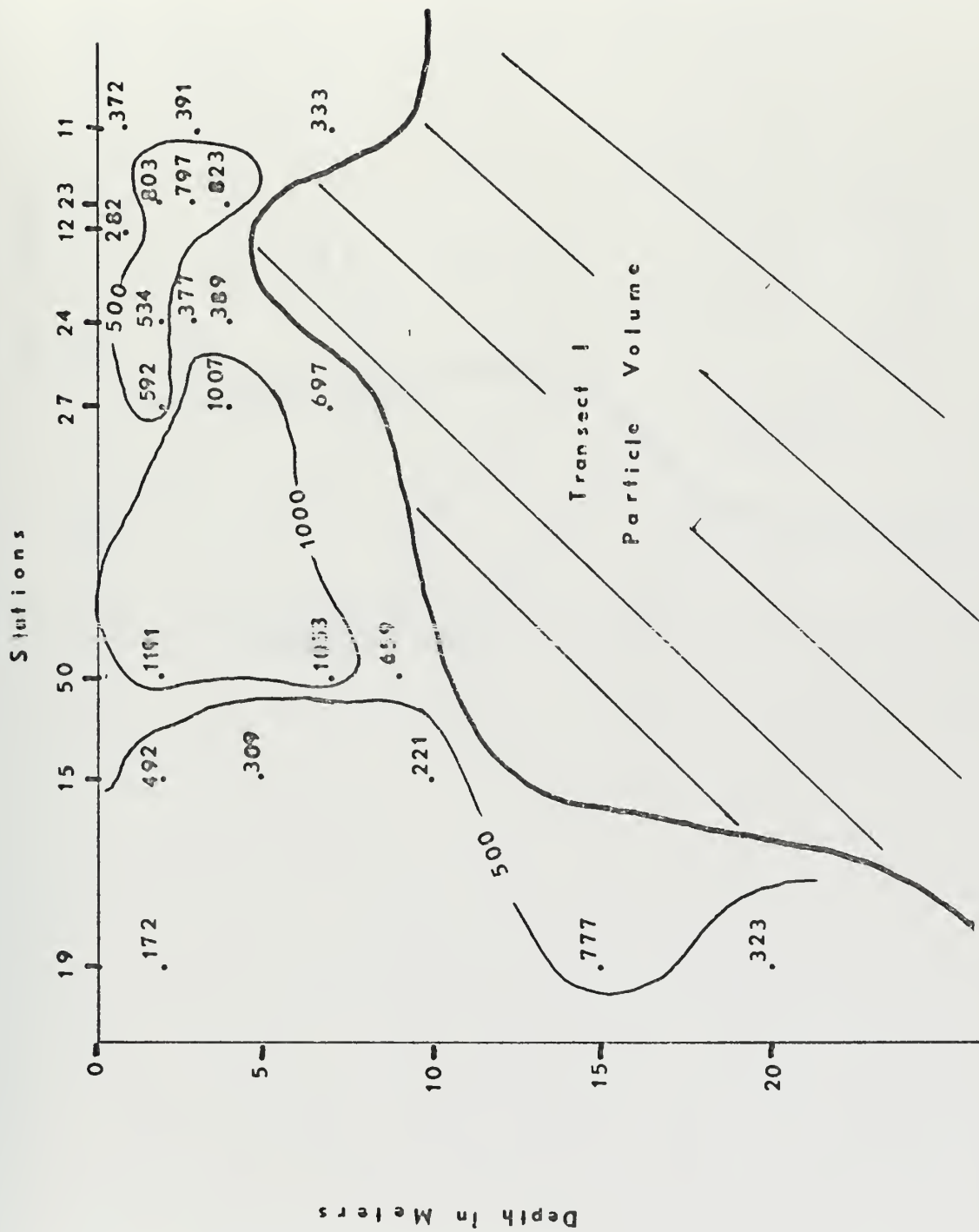


Fig. 14. Transect I Scattering Ratio Contours

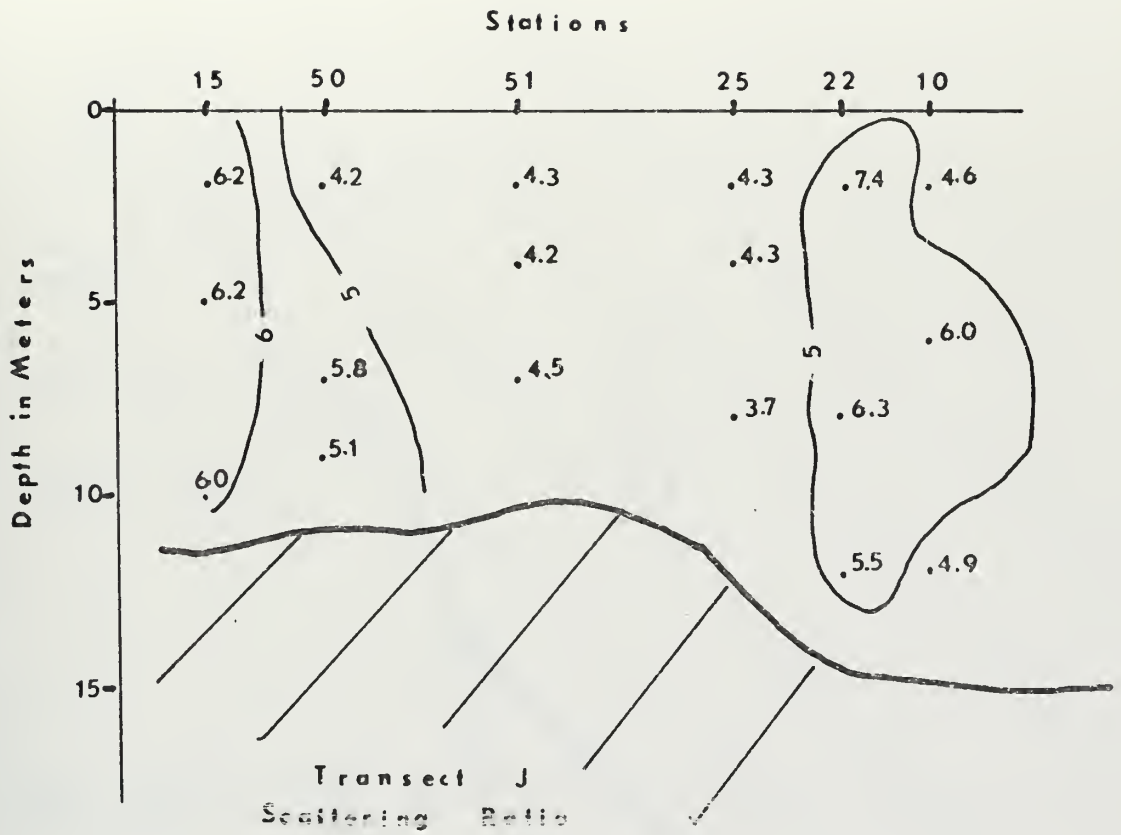


Fig. 15. Transect J Scattering Ratio Contours

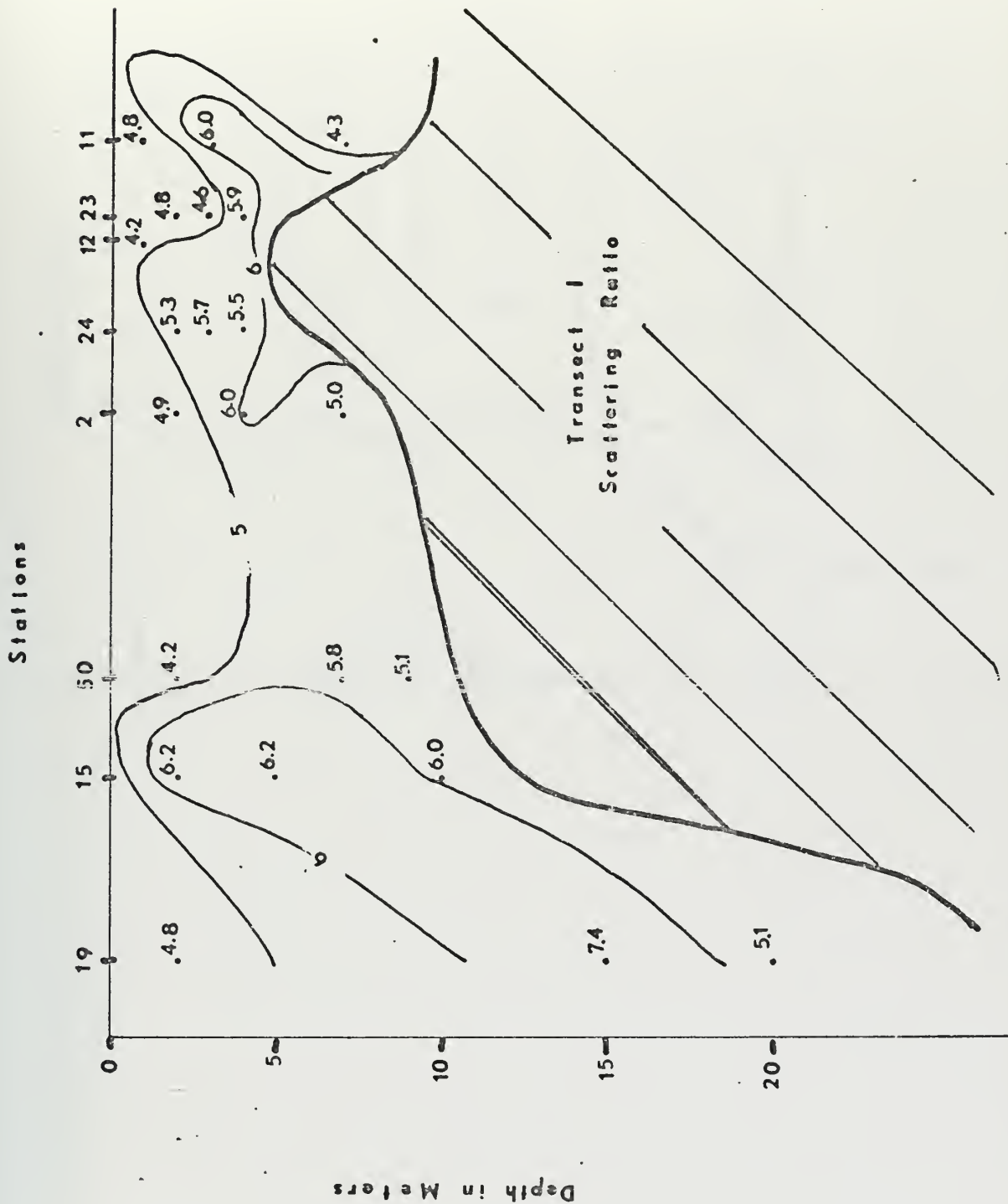


Fig. 16. Transect I Volume Contours

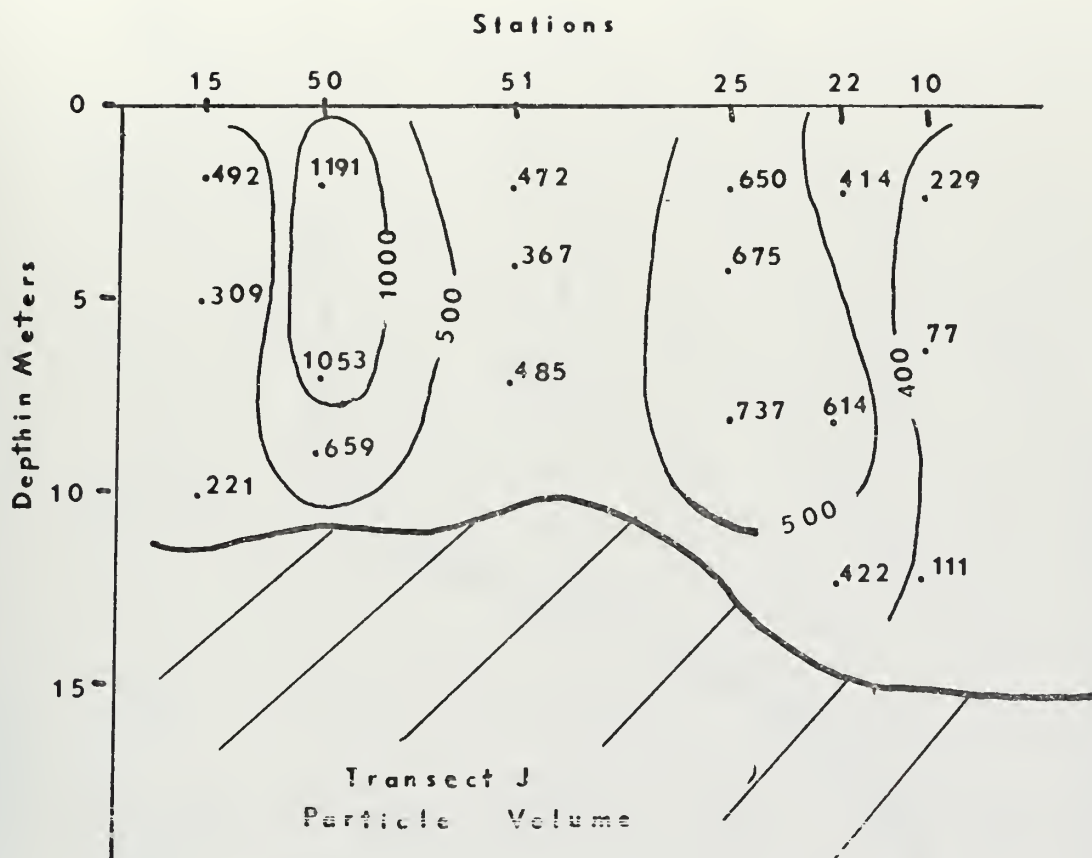


Fig. 17. Transect J Volume Contours

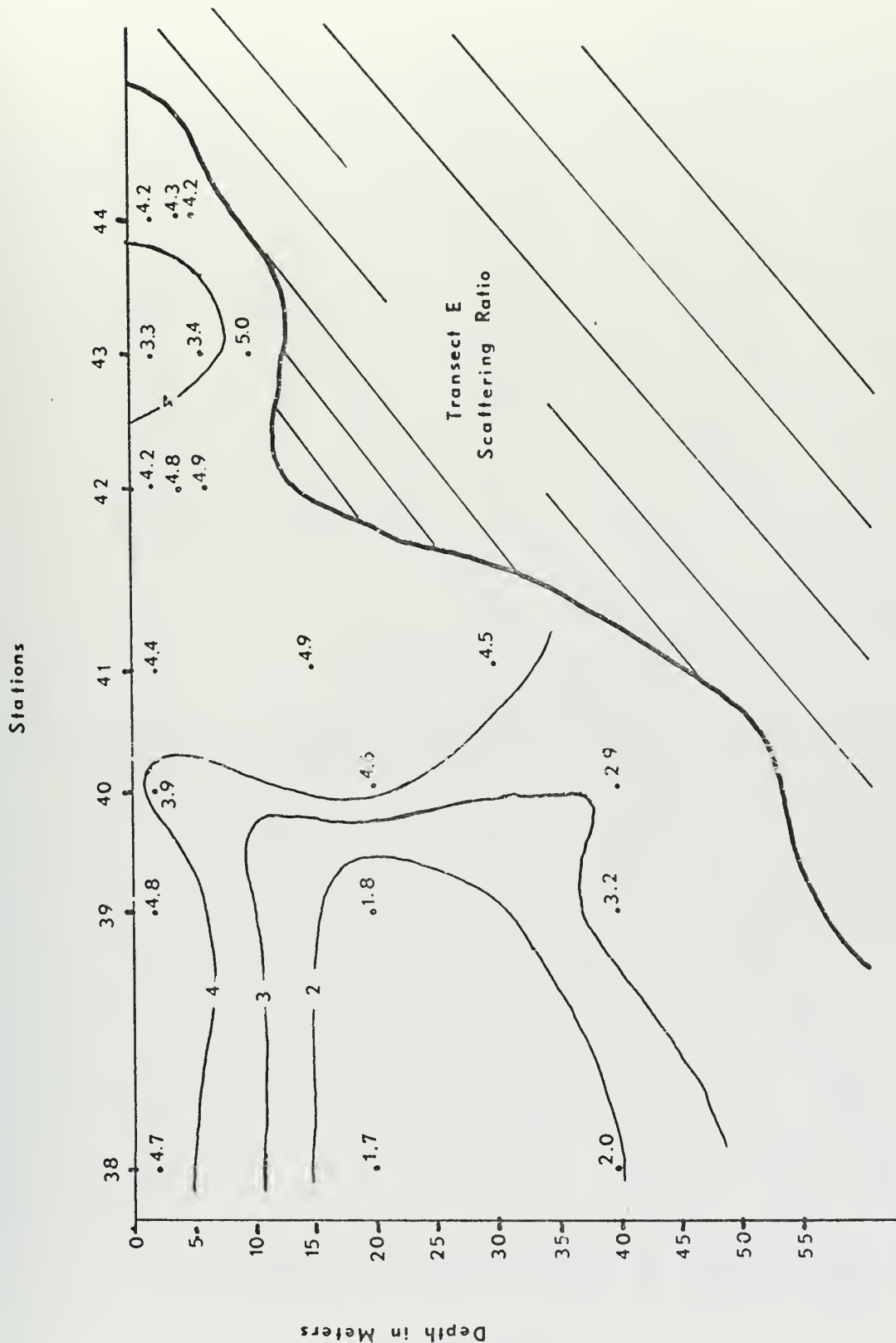


Fig. 18. Transect E Scattering Ratio Contours

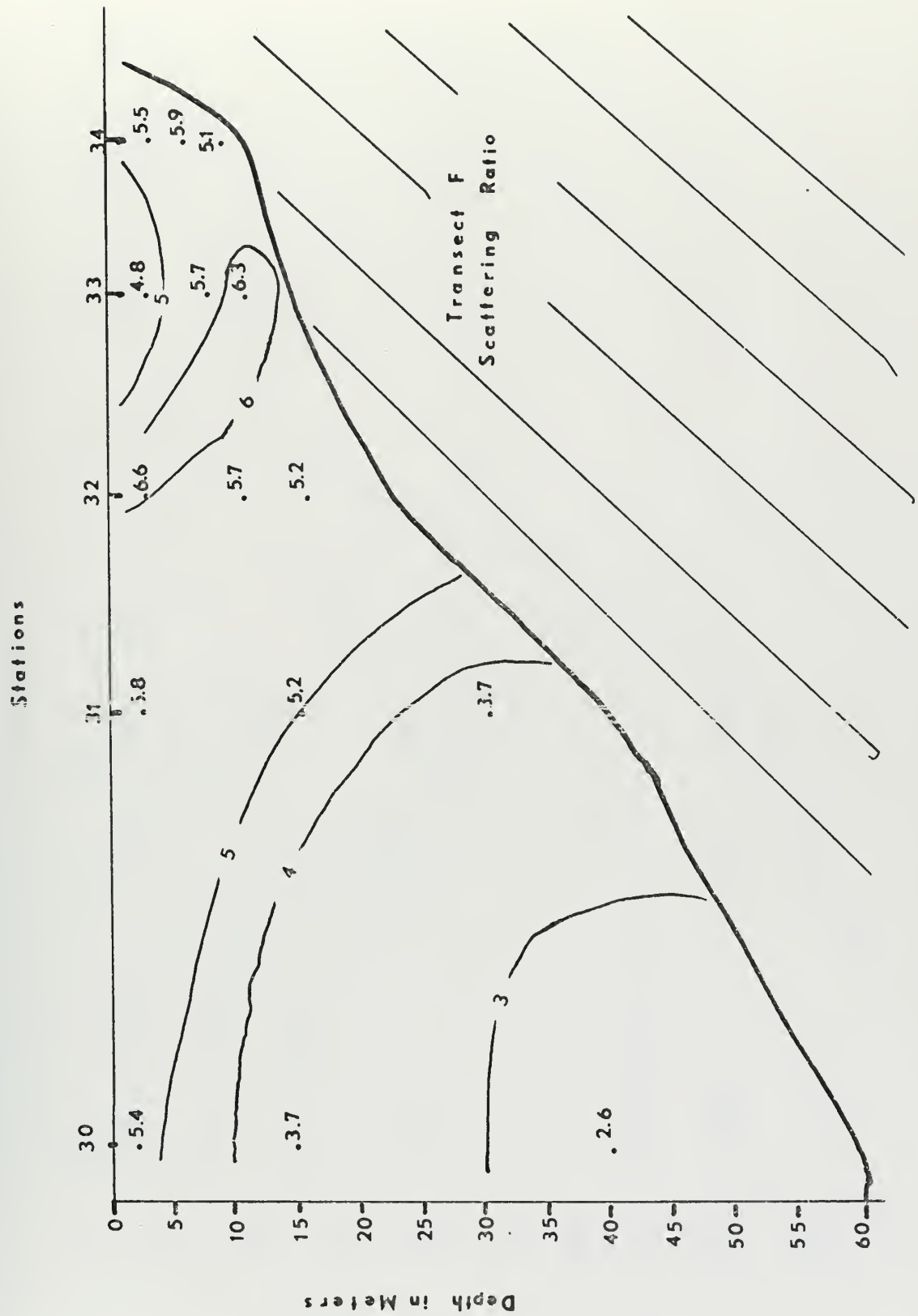


Fig. 19. Transect F Scattering Ratio Contours

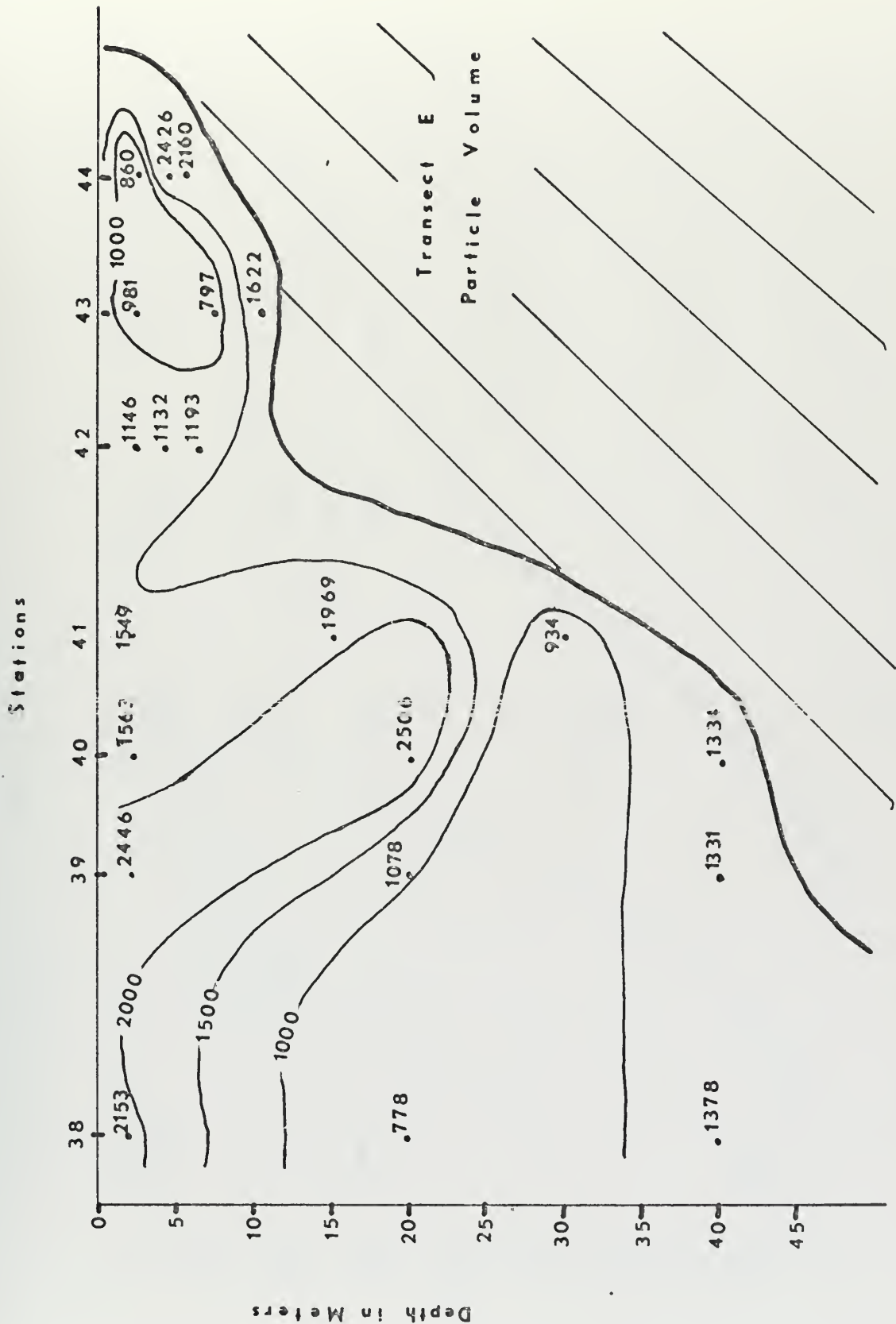


Fig. 20. Transect E Volume Contours

Stations

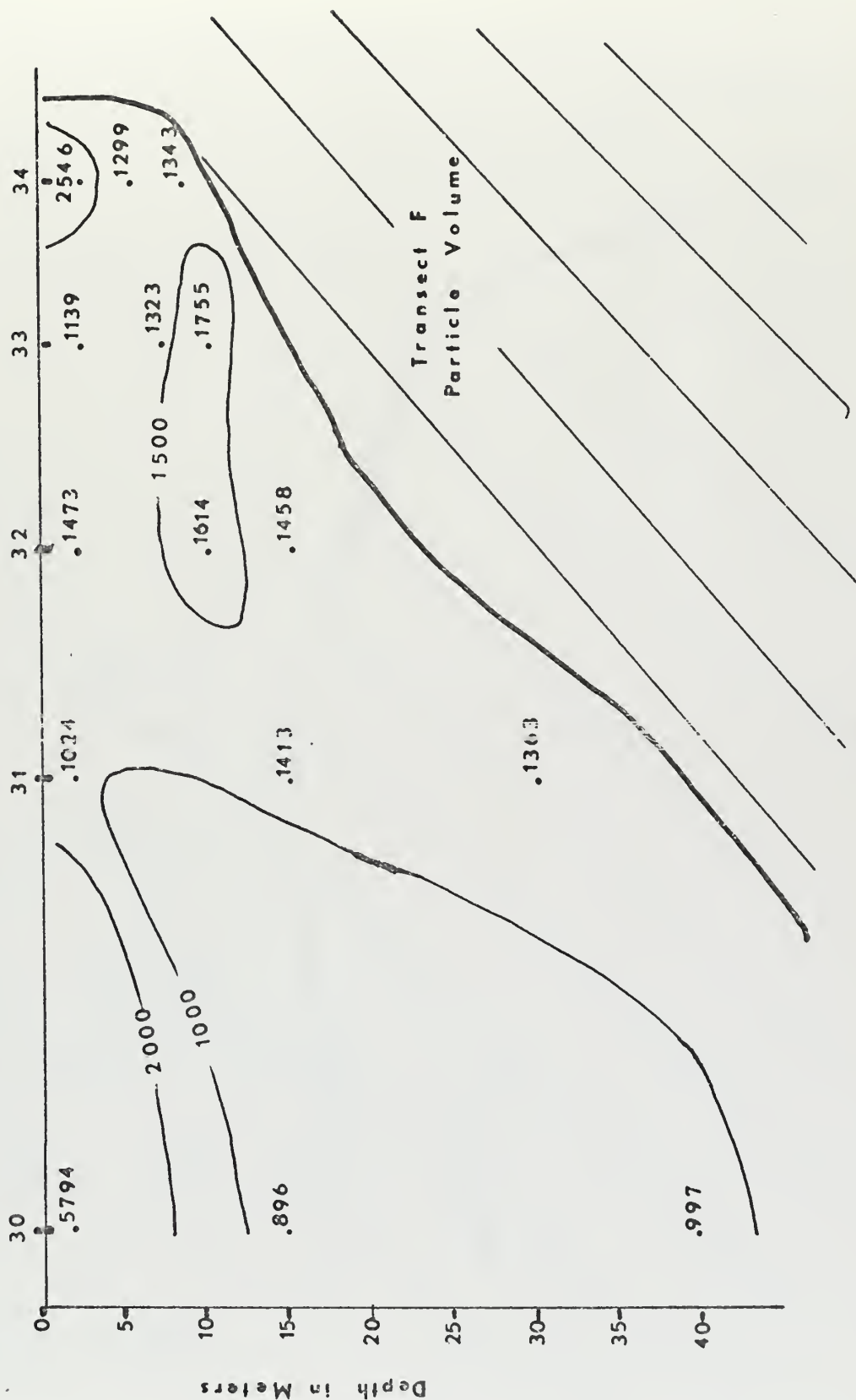


Fig. 21. Transect F Volume Contours

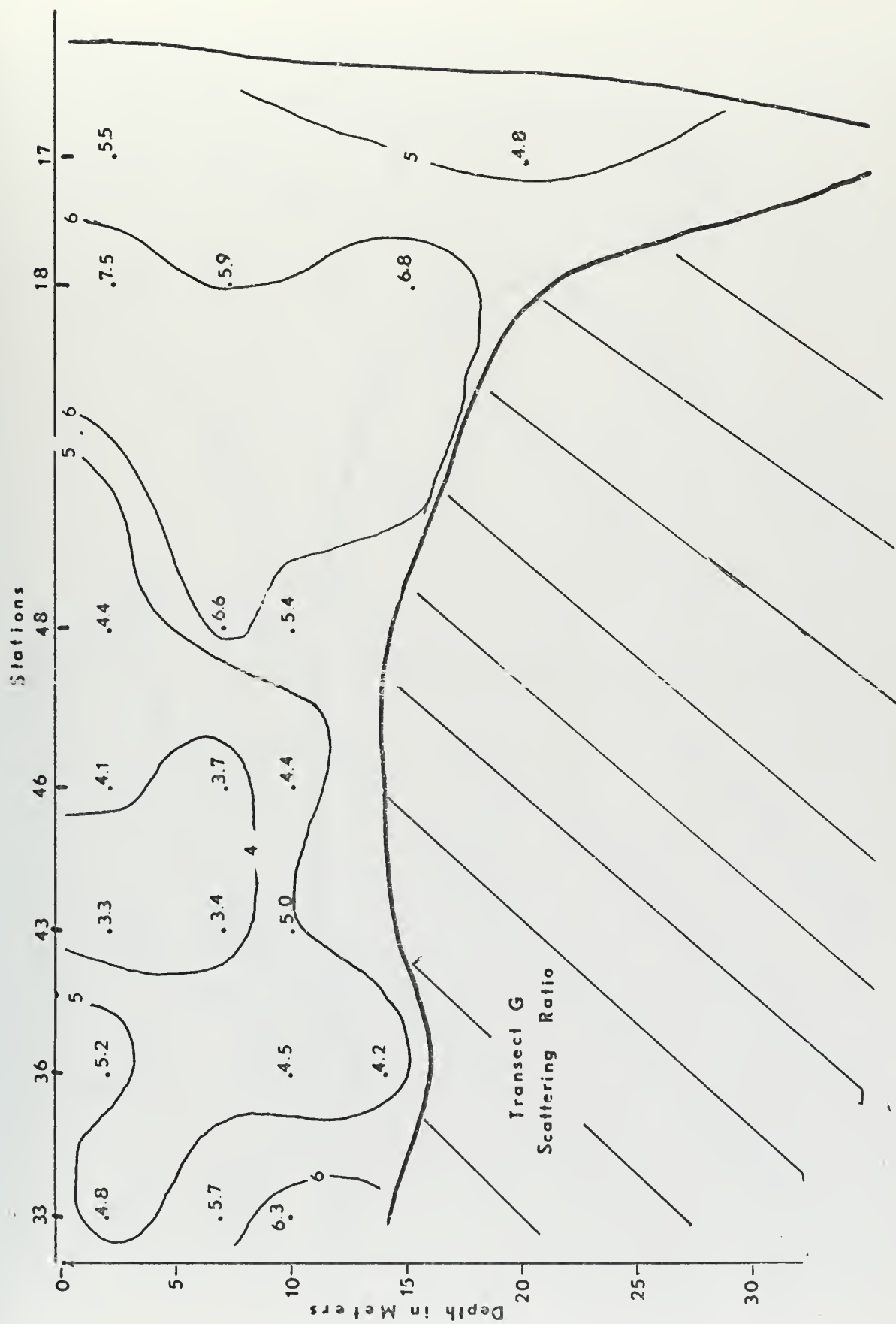


Fig. 22. Transect G Scattering Ratio Contours

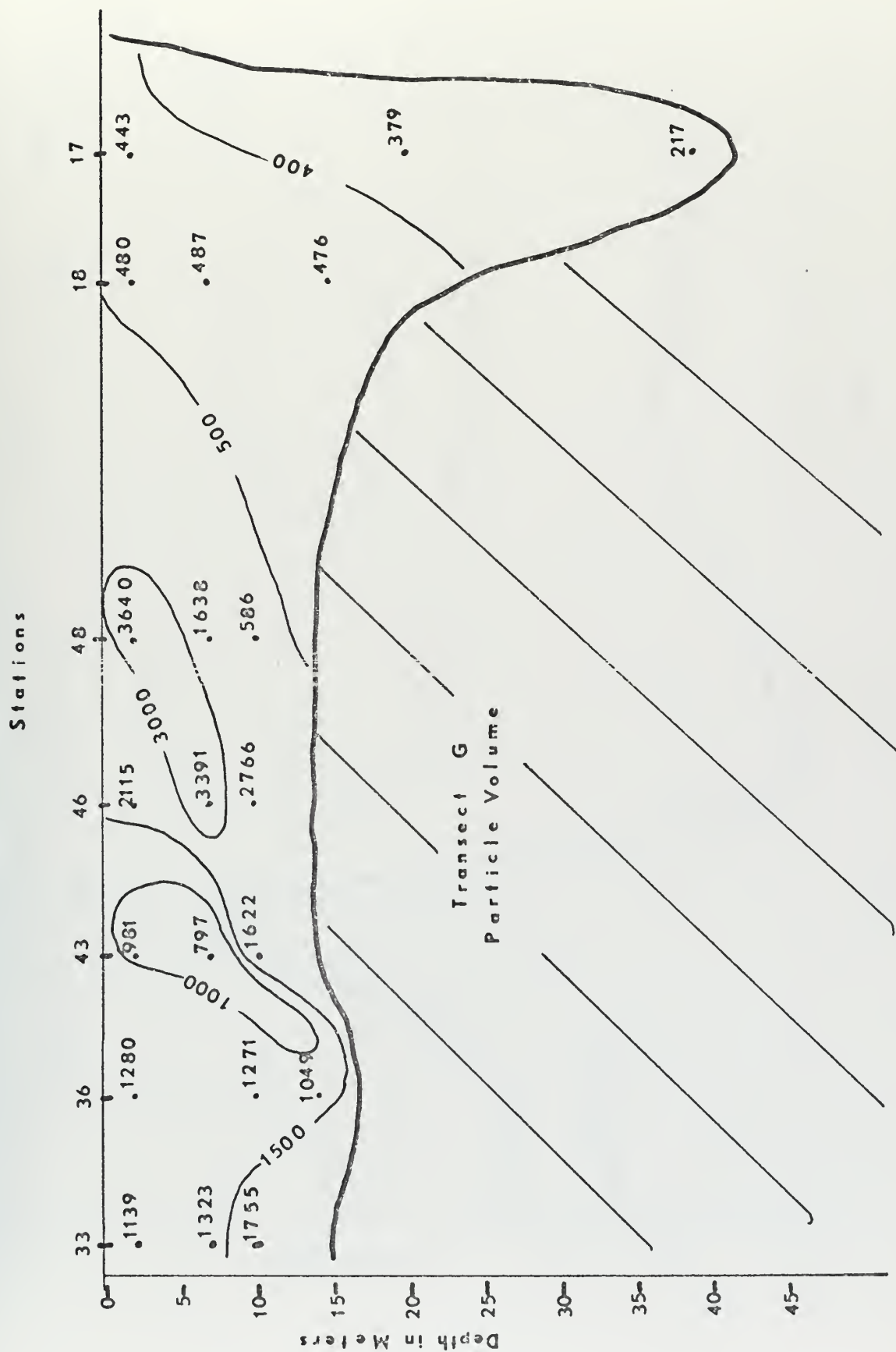


Fig. 23. Transect G Volume Contours

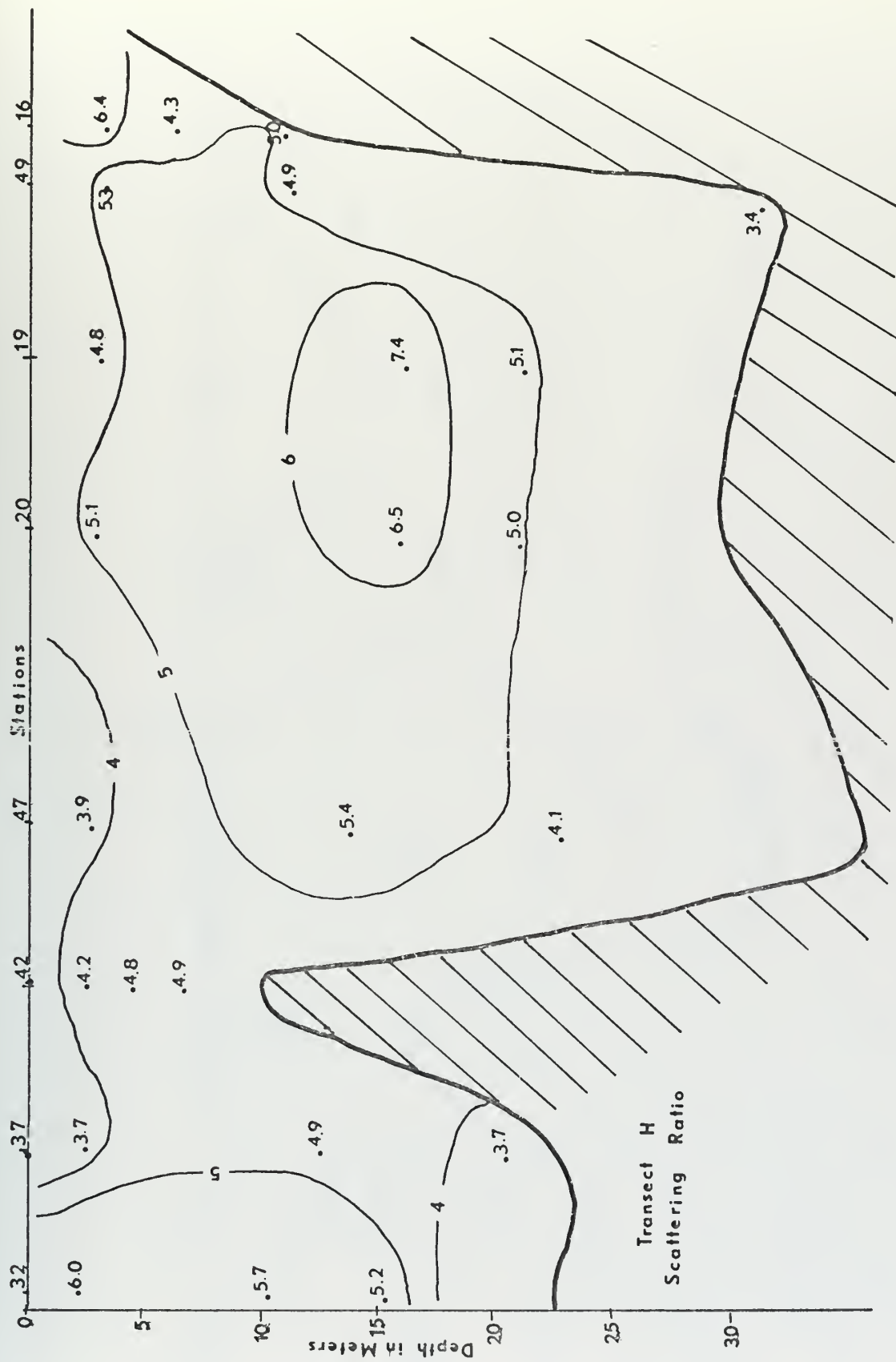


Fig. 24. Transect H Scattering Ratio

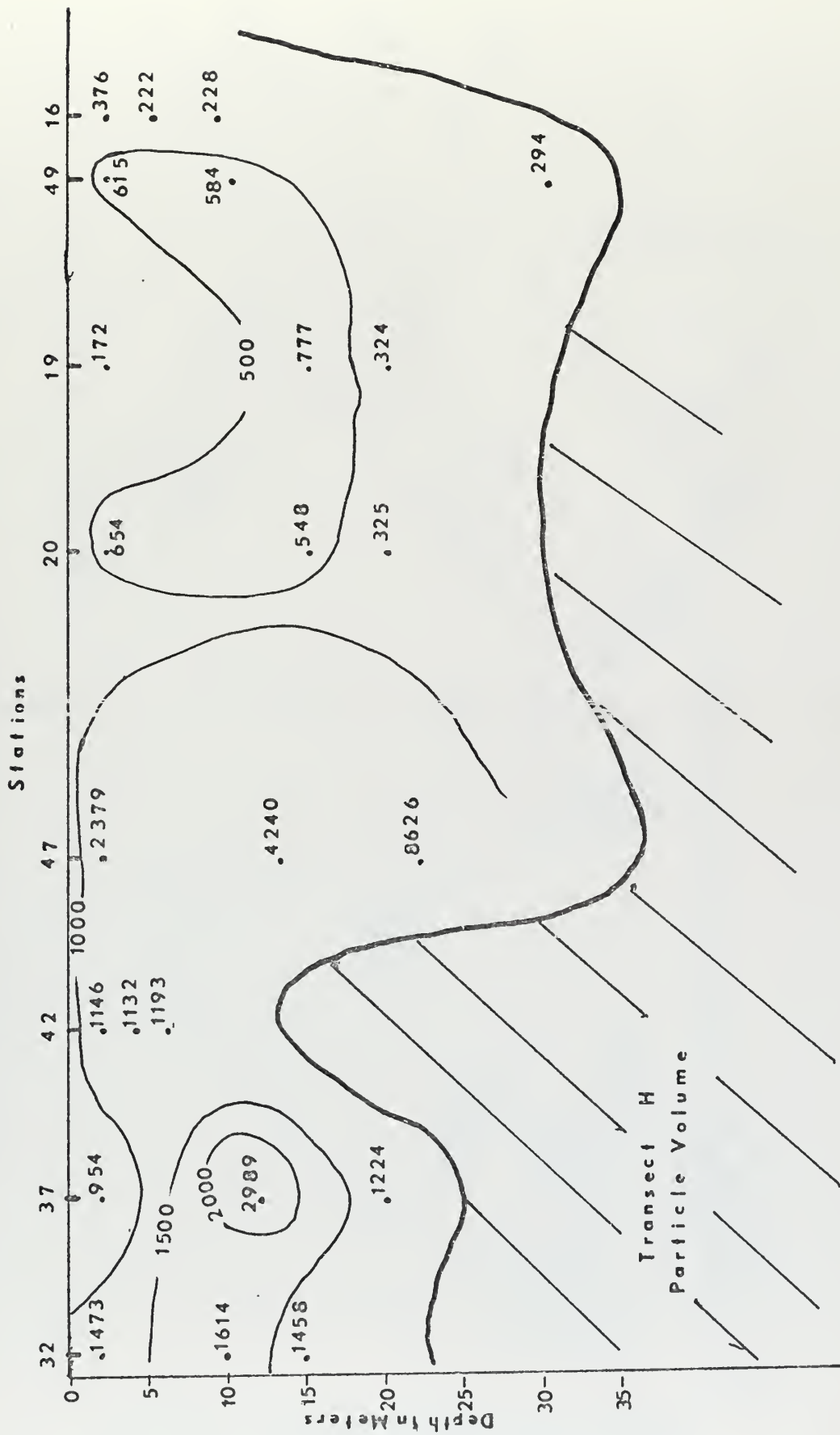


Fig. 25. Transect H Volume Contours

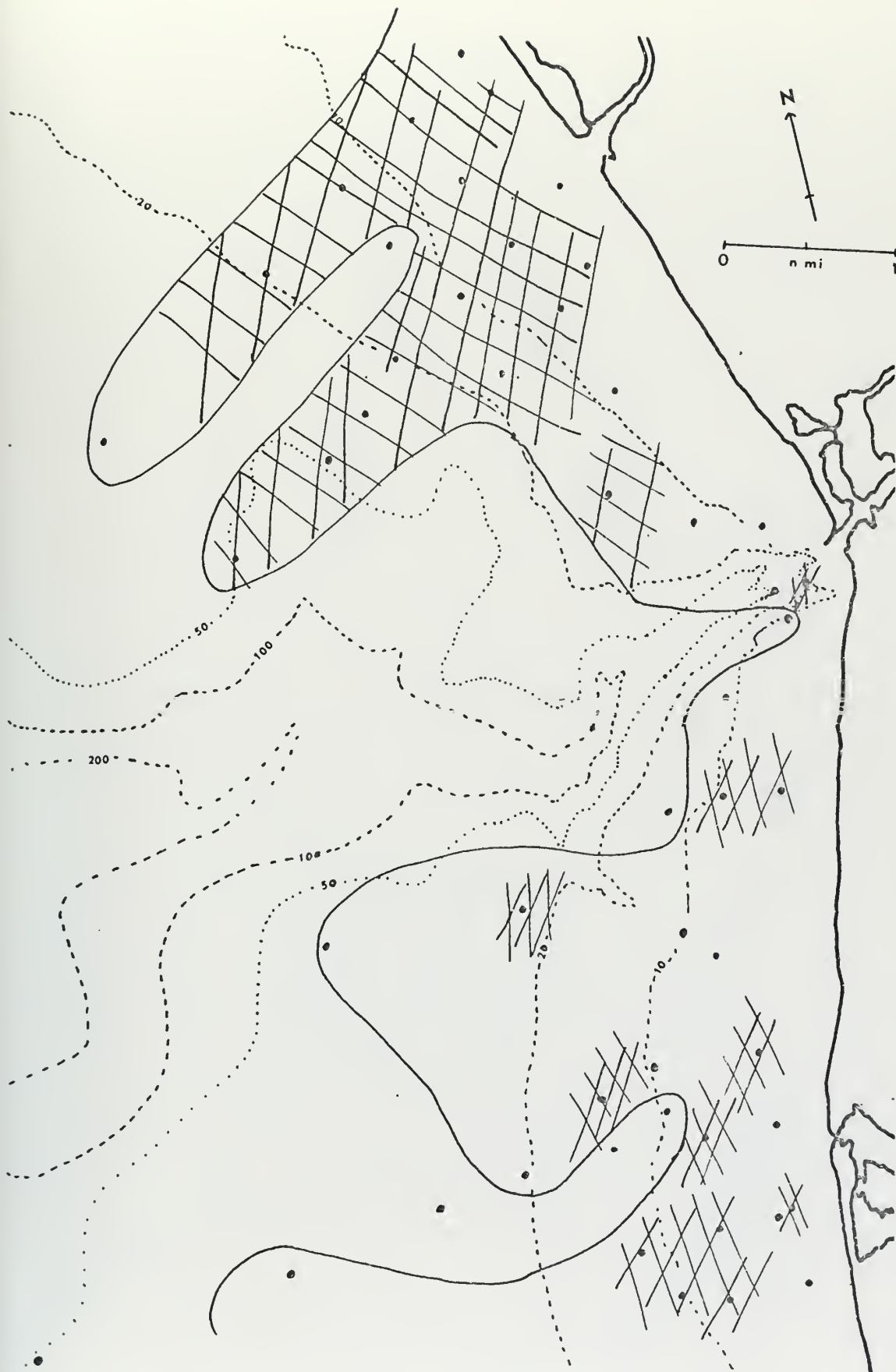


Fig. 26. Montmorillonite Distribution
(cross-hatched area distribution at 2 m)

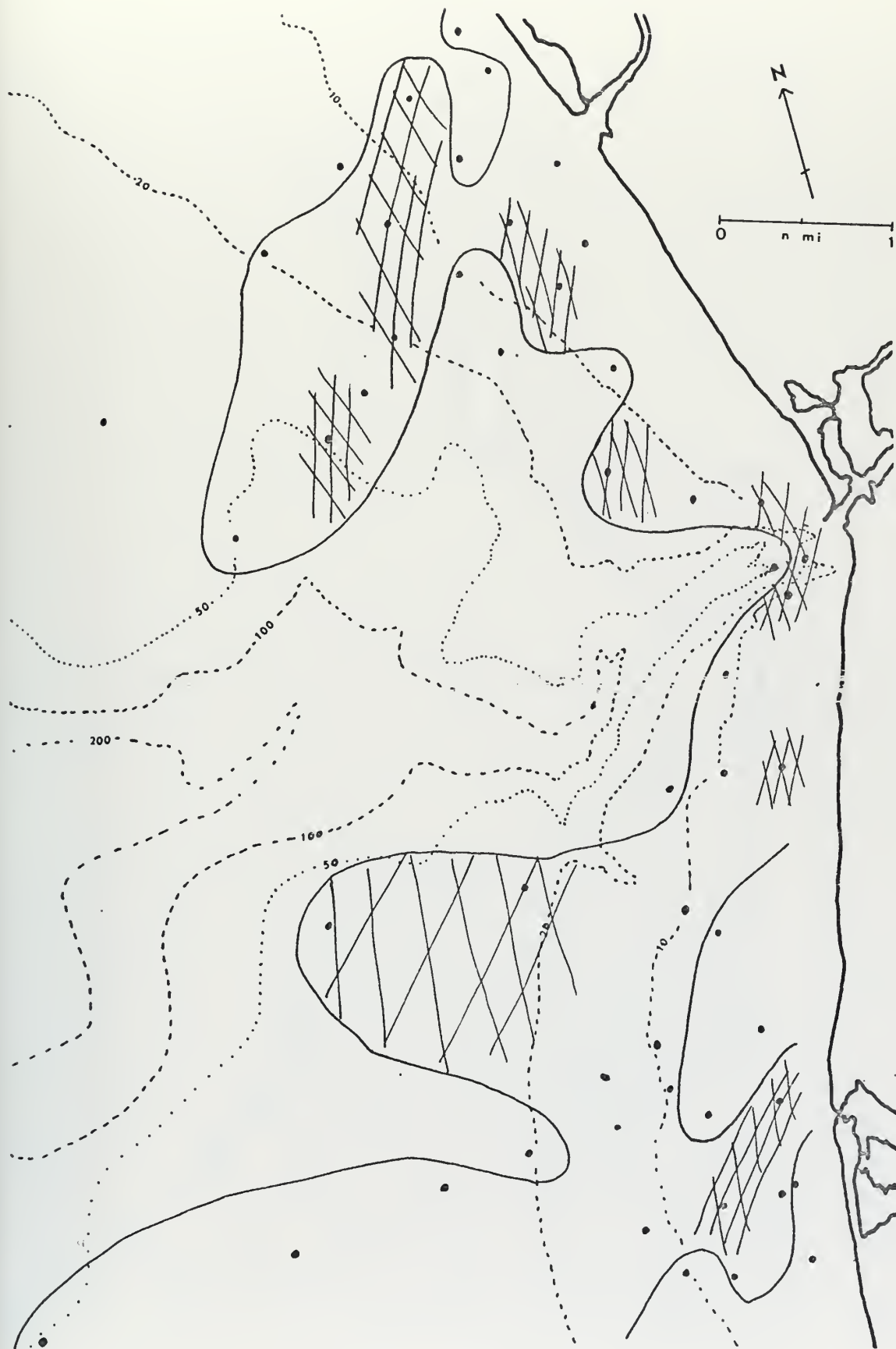


Fig. 27. Kaolinite Distribution
(cross-hatched area distribution at 2 m)

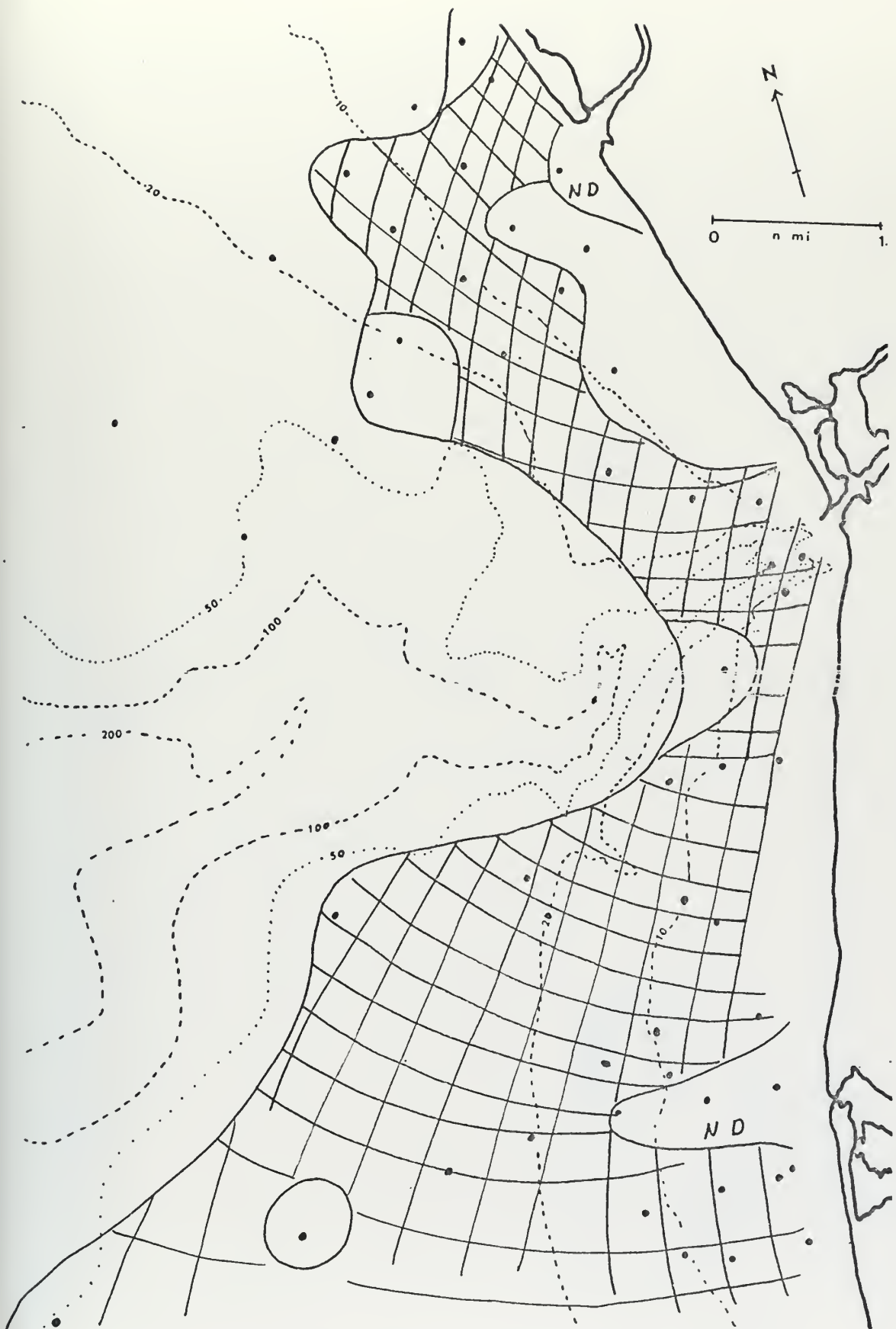


Fig. 28. Muscovite Distribution
(N D: not detected; cross-hatched area distribution at 2 m)



Fig. 29. Illite Distribution
(cross-hatched area distribution at 2 m)



Fig. 30. Hornblende Distribution
(cross-hatched area distribution at 2 m)



Fig. 31. Sphene and Hypersthene (Hp) Distribution
(cross-hatched area distribution at 2 m)

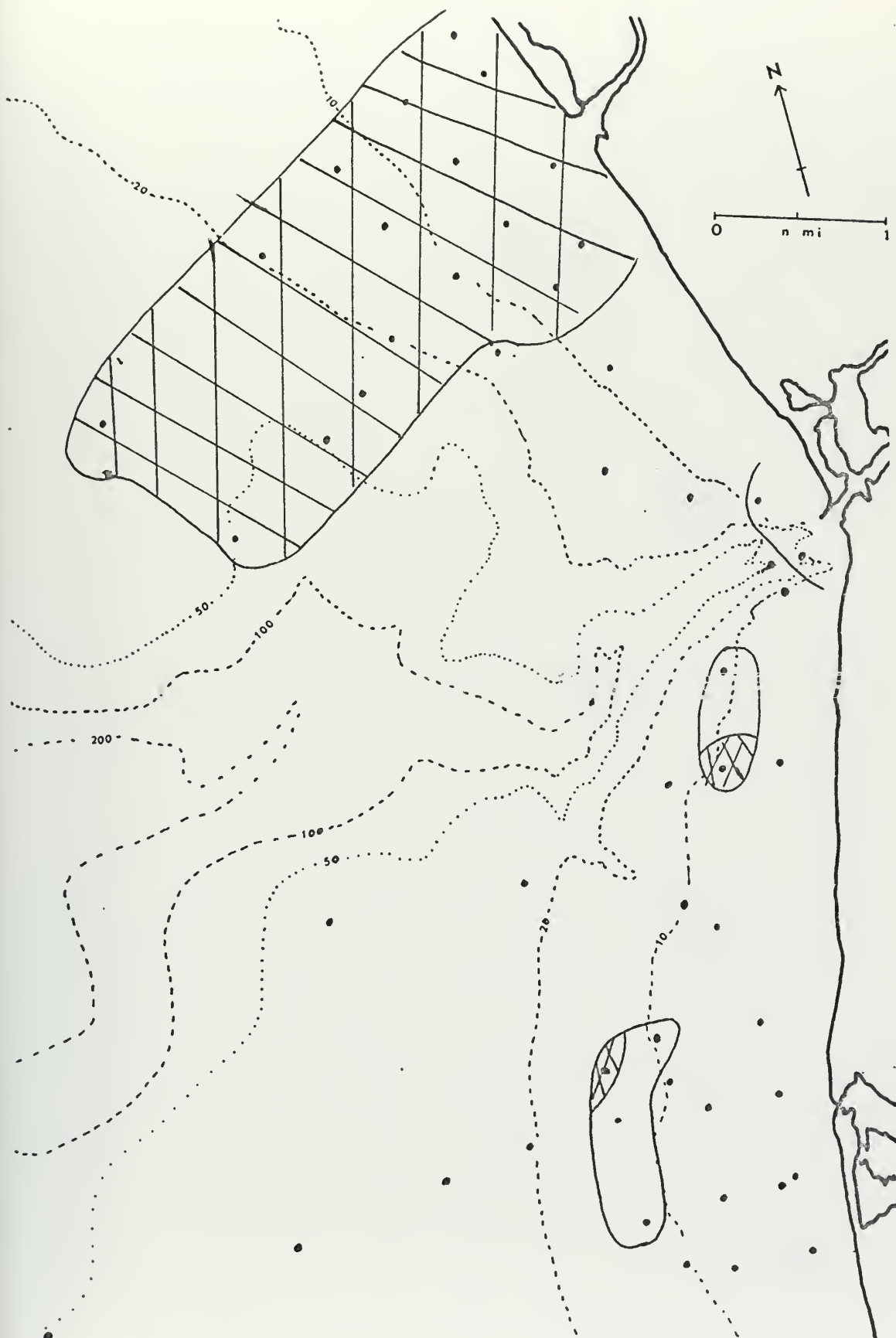


Fig. 32. Jadeite Distribution
(cross-hatched area distribution at 2 m)



Fig. 33. Zircon Distribution
(cross-hatched area distribution at 2 m)

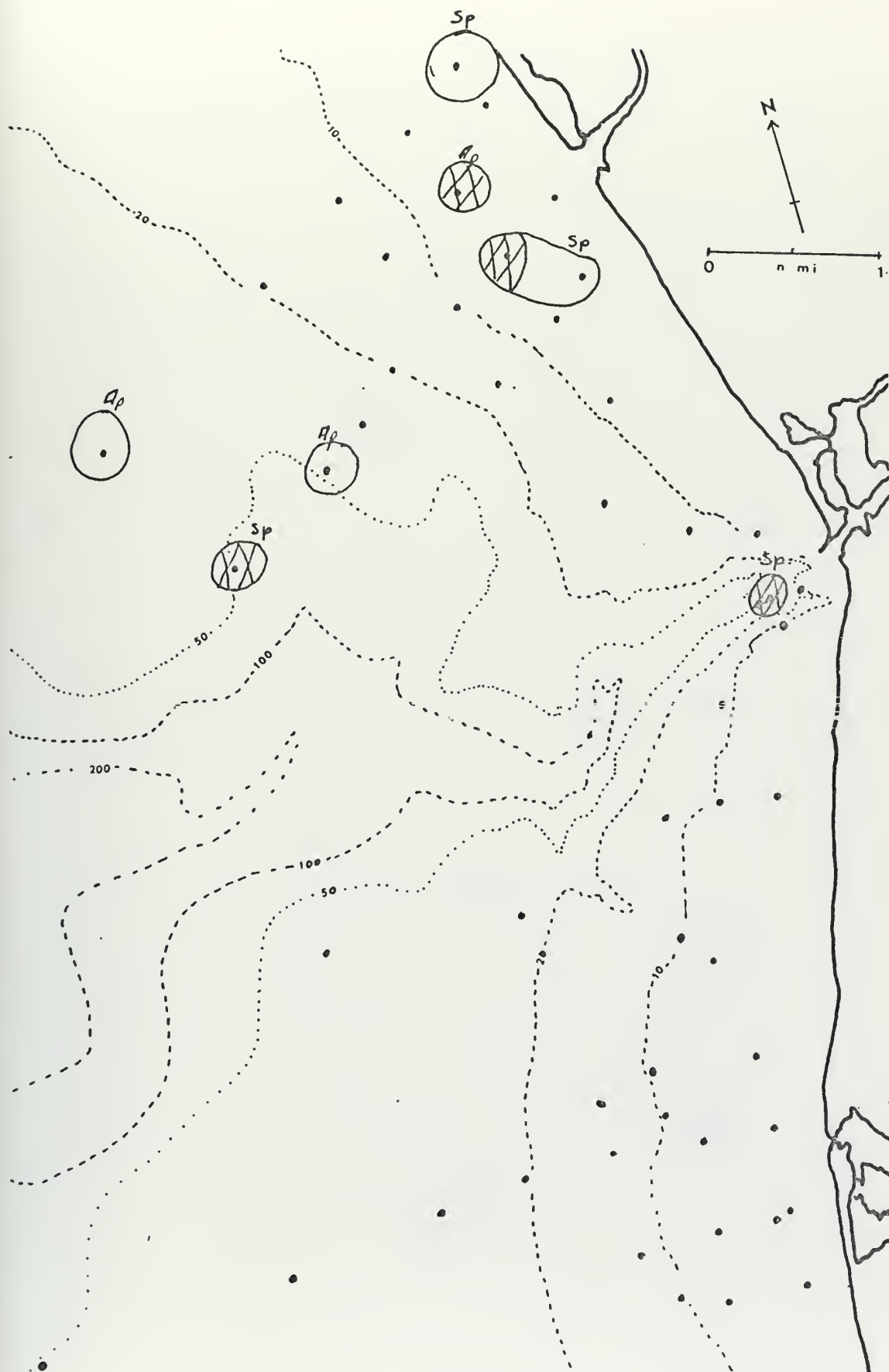


Fig. 34. Serpentine (Sp) and Apatite (Ap) Distribution
(cross-hatched area distribution at 2 m)



Fig. 35. Rutile (R) and Olivine (OL) Distributions
(cross-hatched area distribution at 2 m)



Fig. 36. Epidote Distribution
(cross-hatched area distribution at 2 m)



Fig. 37. Quartz Distribution
(cross-hatched area distribution at 2 m)



Fig. 38. Orthoclase Distribution
(cross-hatched area distribution at 2 m)



Fig. 39. X-ray Intensities
(cross-hatched area "high," "Low" (L) unoutlined area "Medium.")

TABLE 1 STATION DATA

Station Number	Date 1971	Time (PST)	Location	Depth (m)	Sampling Depth (m)	Scattering Ratio (Z)	Particle Volume, (10^3 m^3)	X-ray Intensity *	Minerals **
1	Apr 22	1000	36°44.5'N 121°54.6'W	100	2 30 50	- - -	- - -	L L L	Mu Mu Q
2		1045	36°44.7'N 121°52.5'W	80	2 30 55	- - -	154 - -	L L L	Mu, S Mu, K, M Mu
3		1115	36°44.9'N 121°51.3'W	60	2 30 56	- - -	- - -	M M M	Mu, K, Ol Mu, K, Q Mu, Q, Or
4		1145	35°45.0'N 121°50.6'W	40	2 30 15	- - -	- - 277	M M M	Mu, Q, E Mu, Zr, Q, M, E Mu, Q, E, Or
5		1230	36°45.2'N 121°49.5'W	20	2 10 15 16	- - - -	- 203 - 232	M M L M	Mu, Q, E Mu, K, Or K Mu, K, Q, E, Or
6		1315	36°46.3'N	19	2 10 15 16	- - - -	76 58 120 -	L M M M	Mu, Ol Mu, M Mu, K, E, Or Mu, K, Zr, M, E
7		1345	36°46.6'N 121°50.3'W	50	2 20 35	- - -	- - 40	H M M	Mu, K, E Mu, S, K, E, Ol Mu, S, K, E, Or

Station Number	Date 1971	Time (PST)	Location	Depth (m)	Sampling Depth (m)	Scattering Ratio (Z)	Particle Volume (10 ⁻¹⁴ m ³)	X-ray Intensity*	Minerals **
8	Apr 22	1430	36°46.6'N 121°52.2'W	110	2 30 57	- - -	36 19 24	L L L	Mu,K Mu,K,Ol Mu,K,M,E
9		1510	36°45.3'N 121°55.4'W	125	2 30 50	- - -	- - -	L L L	Mu,K Mu,K,M Mu,K,M
10	May 13	1330	36°44.1'N 121°49.7'W	14	2 6 12	4.6 6.0 4.9	229 77 111	L L L	Mu,K,M Mu,K,M Mu,M,E
11		1400	36°44.0'N 121°48.7'W	8	1 3 7	4.8 6.0 4.2	372 391 333	H H H	Mu,Zr,Q,E,Or Mu,Q,M,Or Q,Or
12		1430	36°44.5'N	4	1	4.2	282	M	Q,M,Or,I
13	June 3	1300	36°47.0'N 121°49.0'W	14	2 14 7	6.9 6.0 6.3	635 602 580	B M M	- Mu,S,Q,E,Or E
14		1330	36°47.0'N 121°48.1'W	7	2 4 7	4.9 5.8 4.7	536 362 411	M M M	Mu,S,K,Q,M,E,Or Mu,K,Or Mu,Q
15		1400	36°47.6'N 121°48.4'W	10	2 10 5	6.2 6.0 6.2	492 221 309	L M L	Hp,Or Mu,K,M,E,Or,J Mu,K,M,E,Or

Station Number	Date 1971	Time (PST)	Location	Depth (m)	Sampling Depth (m)	Scattering Ratio (Z)	Particle Volume $\left(\frac{V}{m^3}\right)$	X-ray Intensity *	Minerals **
16	June 3	1430	36°48.0'N 121°47.8'W	9	2 9 5	6.4 5.0 4.3	376 228 222	M M M	Mu, K, Q, E, Or, H Mu, S, K, E, Or Mu, K, Q
17		1445	36°48.2'N 121°47.6'W	39	2 39 20	5.5 5.8 4.8	443 217 379	L M M	Mu, K, Q, M, Or Mu, K, Q, E, Or Mu, M, E, Or, J
18		1530	36°48.6'N 121°47.8'W	20	2 7 15	7.5 5.9 6.8	480 487 476	L M L	Mu, K, Q, Or, Ol Mu, S, K, Q, M, Or, Ol Mu, K, M, J
19		1600	36°48.7'N 121°48.4'W	30	2 15 20	4.8 7.4 5.1	172 777 324	L M H	Mu, Or Mu, K, M, E, Or, J Mu, S, K, M, Or, J
20		1630	36°48.9'N 121°49.0'W	28	2 15 20	5.1 6.5 5.0	654 548 325	L L L	Mu, K, M, Or, J K, Q, M, Or, I Mu, M, Or
21	June 10	0930	36°44.4'N 121°49.9'W	30	2 13 20	5.2 5.5 5.0	103 59 88	L L L	Mu, S, M Mu, K, M, Or, J Mu, K, M, I
22		0940	36°44.5'N 121°49.3'W	14	2 8 12	7.4 6.3 5.5	414 614 422	M M M	Mu, K, M, I Mu, K, I Mu, I
23		0950	36°44.5'N 121°48.7'W	4	2 4 3	4.8 5.9 4.6	804 823 797	M M M	Mu, Or, I Mu, K, M, Or, I Mu, K, Or, I

Station Number	Date 1971	Time (FST)	Location	Depth (m)	Sampling Depth (m)	Scattering Ratio (Z)	Particle Volume (10 ⁻¹⁴ m ³)	X-ray Intensity *	Minerals **
24	June 10	1000	36°45.0'N 121°48.7'W	4	2 4 3	5.3 5.5 5.7	534 389 377	H L L	Mu, K, Or Mu, K, M Mu, E, Or, H
25		1015	36°45.0'N 121°49.2'W	8	2 4 8	4.3 4.3 3.7	650 675 737	L L L	Mu, M Mu Mu, M, I
26		1050	36°45.5'N 121°49.4'W	14	2 8 12	5.2 4.8 4.1	692 893 348	L L L	Mu, S Mu, S, K, M, J, I, H Mu, M, Or, J
27		1105	36°45.0'N 121°48.7'W	7	2 4 7	4.9 6.0 5.0	331 1007 697	L L L	Mu, S, M S, M, H Mu, M, E
28		1030	36°45.1'N 121°50.0'W	16	2 14 16	4.9 4.7 4.8	463 109 227	L L L	H K, Or, J K, J, I, H
29		1040	36°45.4'N 121°49.9'W	18	2 10 18	5.1 5.2 4.3	852 736 105	L L L	Mu, M, Or, J, H Mu, S, K, M, Or, J Mu, S, M, Or, J, H
30	June 16	1030	36°49.9'N 121°52.5'W	60	2 15 40	5.4 3.7 2.6	5794 896 997	B L L	- S, M, J, H M, Ap, R, J
31		1100	36°50.7'N 121°51.1'W	40	2 15 30	5.8 5.2 3.7	1024 1413 1363	L L L	Mu, M, J Mu, K, M, J S, M, J, H

Station Number	Date 1971	Time (PST)	Location	Depth (m)	Sampling Depth(m)	Scattering Ratio (Z)	Particle Volume (v) ($10^{-14} m^3$)	X-ray Intensity *	Minerals **
32	June 16	1115	36°51.2'N 121°50.4'W	22	2 10 15	6.0 5.7 5.2	1473 1614 1458	L B L	Mu,S,M,J - M
33		1130	36°51.5'N 121°49.9'W	14	2 7 10	4.8 5.7 6.3	1139 1323 1755	M L L	S,K,M,J,H S,M,J M,Or,I
34		1150	36°51.8'N 121°49.4'W	10	2 5 8	5.5 5.9 5.1	2546 1299 1343	B L M	- Mu,S,K,M,J Mu,S,K,M,J,Sp
35		1200	36°51.5'N 121°49.2'W	6	2 3 4	5.1 5.1 4.9	1231 1195 1679	L L L	Mu,S,K,M,J Mu,S,M,J Mu,S,M,E,J
36		1215	36°51.0'N 121°49.5'W	16	2 10 14	5.2 4.5 4.2	1280 1271 1049	M M M	Mu,S,M,J,Hp Mu,S,M,J Mu,S,M,Or,J
37		1225	36°50.8'N 121°50.2'W	24	2 12 20	3.7 4.9 3.7	954 2989 1224	M M B	Mu,K,M,J,H Mu,K,M,J,H -
38		1335	36°49.0'N 121°51.8'W	100	2 20 40	4.7 1.7 2.0	2153 778 1378	H H H	S,K,M,J S,K,M S,M,J,Sp
39		1315	36°49.5'N 121°51.0'W	100	2 20 40	4.8 1.8 3.2	1446 1079 1331	H H M	S,K,M,J,H,Sp S,K,Zr,M,E,J S,M,Ap,J

Station Number	Date 1971	Time (PST)	Location	Depth (m)	Sampling Depth (m)	Scattering Ratio (Z)	Particle Volume (10 ⁻¹⁴ m ³)	X-ray Intensity *	Minerals **
40	June 16	1300	36°49.8'N 121°50.7'W	60	2 20 40	3.9 4.6 2.9	1563 2506 1334	L L L	R Mu, M, J S, K, J, H
41		1445	36°50.0'N 121°50.3'W	40	2 15 30	4.4 4.9 4.5	1549 1869 938	H M H	S, K, M, J, H Mu, M, J, H S, K, Q, M, J, H
42	June 18	0930	36°50.4'N 121°49.3'W	6	2 6 4	4.2 4.9 4.8	1146 1193 1132	L M M	Mu, S, M, J S, M, I Mu, S, M, E
43		1005	36°50.7'N 121°49.3'W	14	2 7 10	3.3 3.4 5.0	981 797 1622	L H M	K, Zr, M, J, H, Sp S, M, J, I Mu, S, K, M, J, I
44		1020	36°50.9'N 121°48.8'W	6	2 4 5	4.2 4.3 4.2	860 2426 2160	M M M	Q, Or, J S, K, Q, M, Or, J S, K, M, E, Or, J, H
45		1030	36°50.4'N	6	2 4 5	4.2 4.4 3.5	3834 1179 1789	M M M	Q, H, Or, M, J Mu, K, S, M, Ol, H, Or, S, K, E, Or, M, J, Zr, Q
46		1045	36°50.2'N 121°49.0'W	14	2 7 10	4.1 3.7 4.4	2115 3391 2766	H M M	Mu, S, K, Zr, M, E, J, I Mu, Zr, Or Mu, S, K, M, E, Or, J
47		1100	36°49.8'N 121°49.5'W	36	2 13 22	3.9 5.4 4.1	2379 4240 8626	L L M	Mu, Q, M Mu, Q, Or Mu, Q, H

Station Number	Date 1971	Time (PST)	Location	Depth (m)	Sampling Depth (m)	Scattering Ratio (Z)	Particle Volume $(10^{-14} \frac{V}{m^3})$	X-ray Intensity *	Minerals **
48	June 18	1110	36°49.5'N 121°48.7'W	14	2 7 10	4.4 6.6 5.4	3640 1638 586	L M L	R, H Mu, Q, M Mu, Q
49		1140	36°48.2'N 121°47.9'W	30	2 10 30	5.3 4.9 3.4	615 585 294	H M M	Mu, Q, Ap, E, Or, Sp Q, Ol, E, Or, H Mu, Q, M, Or, I
50		1155	36°47.0'N 121°48.6'W	9	2 7 9	4.2 5.8 5.1	1191 1053 658	M M L	Mu, Q, M, Or Mu, S, K, Q, M Mu, Or, H
51		1215	36°46.1'N 121°48.9'W	7	2 7 4	4.3 4.5 4.2	472 485 367	L M L	Mu, Or, J Mu, Zr, Or, H Mu, M, Or
52		1300	36°44.1'N 121°49.7'W	8	2 8 4	4.3 4.5 4.6	798 752 900	L L L	Mu, S, M, I Mu, Or, I Mu, S, M

* Intensity classification "low" (L), "medium" (M), "high" (H), "background" (B)

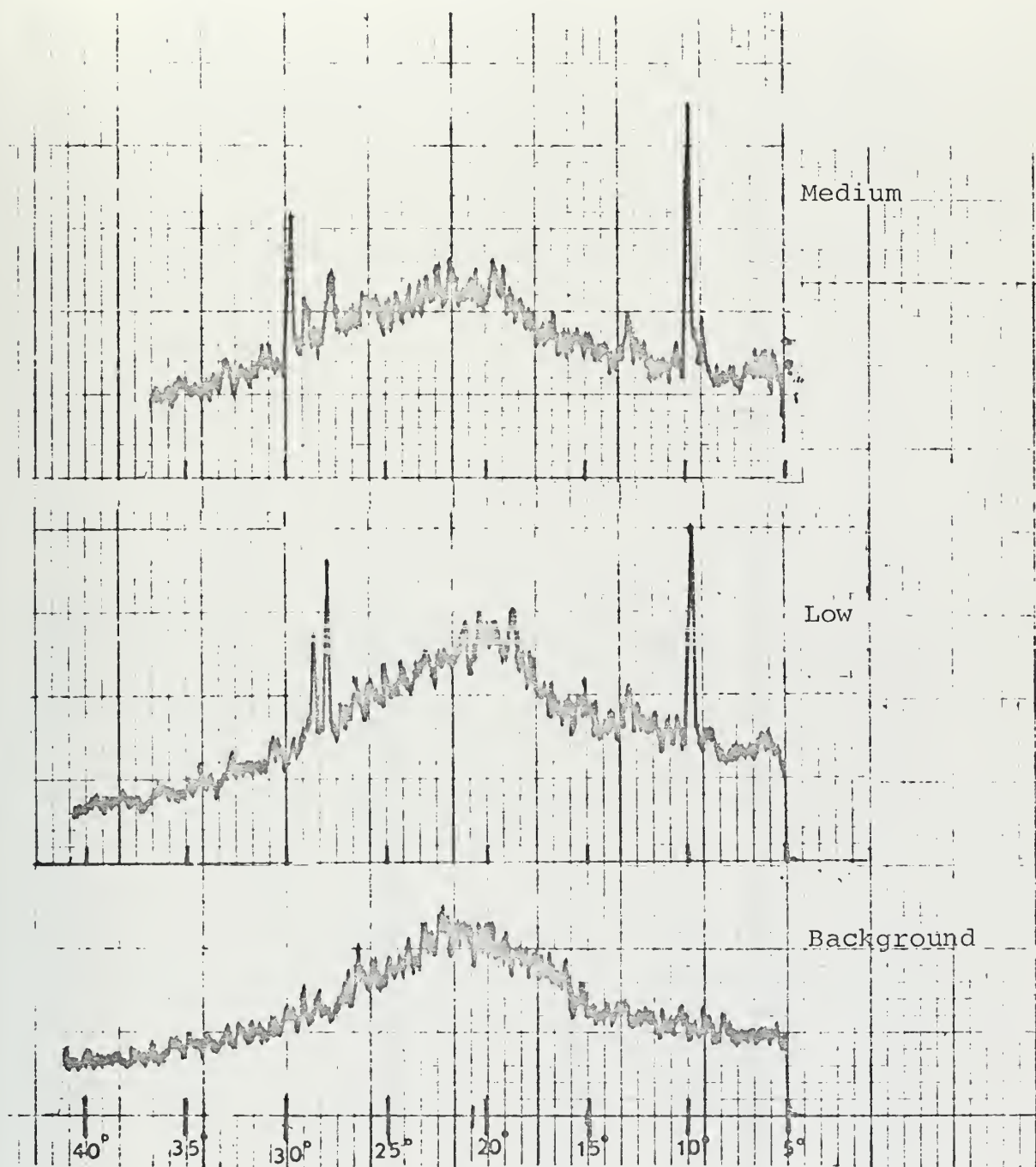
** Mineral abbreviations used: muscovite (Mu), kaolinite (K), quartz (Q), epidote (E), orthoclase (Or), apatite (Ap), sphene (S), hornblende (H), olivine (Ol), illite (I), Montmorillonite (M), jadeite (J), hypersthene (Hp), zircon (Zr), serpentine (Sp).

TABLE II PAJARO and SALINAS RIVER
STREAM DISCHARGE DATA*

	Salinas River	Pajaro River
Winter 1970	82,015	66,621
March 1971	2,619	1,899
April 1971	192	1,252
May 1971	136	708
June 1971	no data	373

*data in ft³/sec

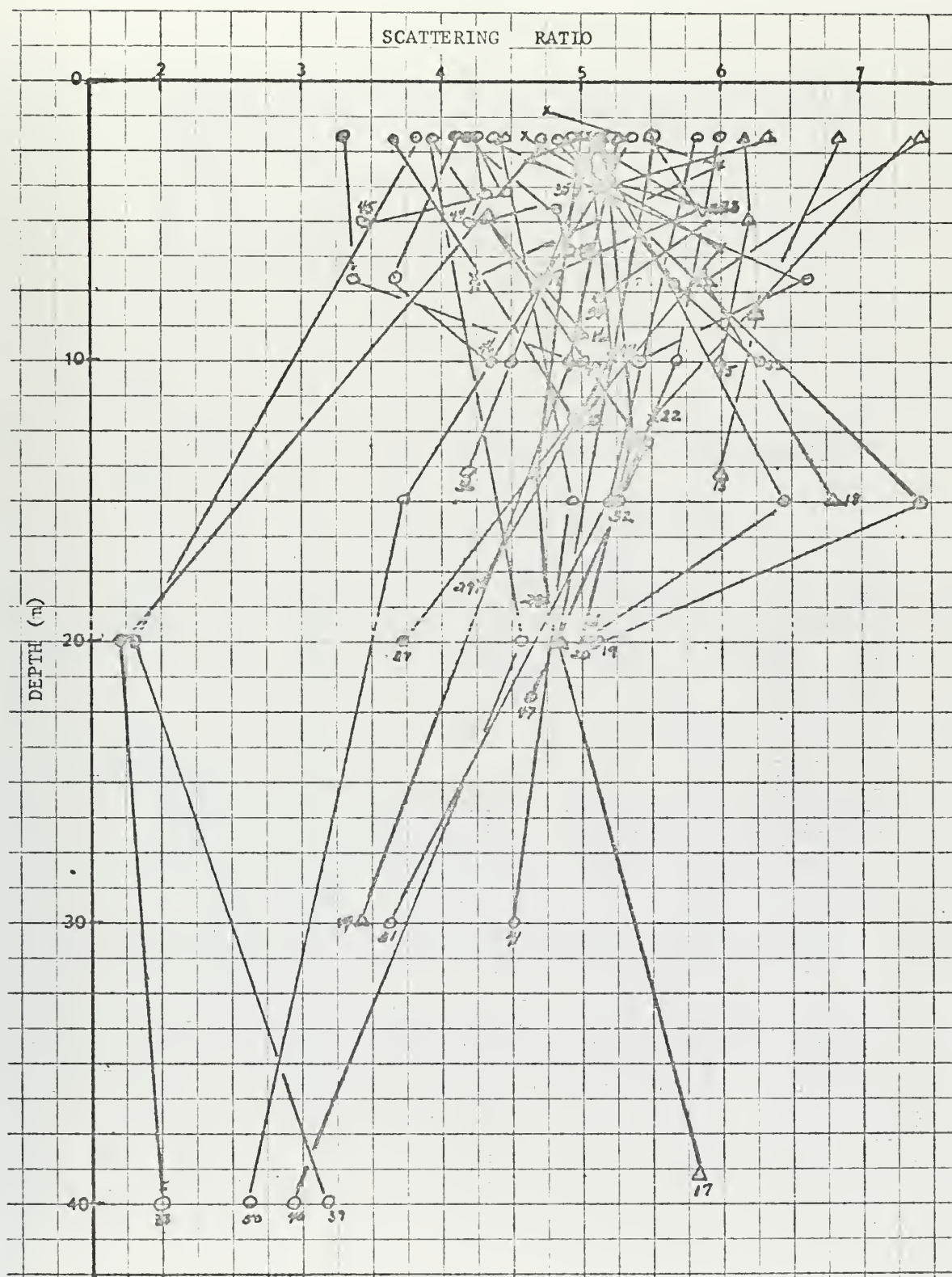
APPENDIX



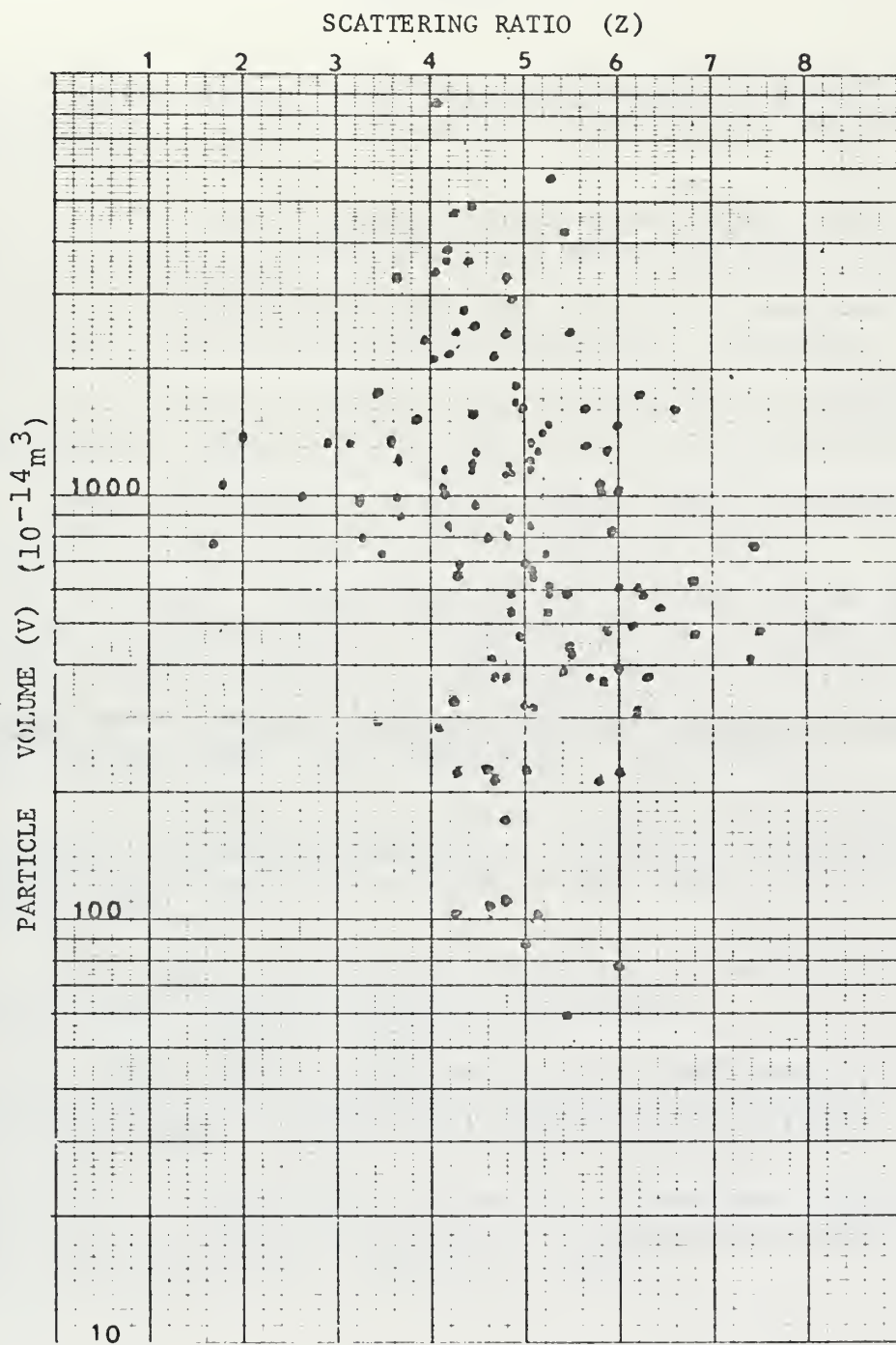
Characteristic X-ray intensities



Characteristic "High" X-ray intensity



Scattering Ratio as a Function of Depth



Scattering ratio as function of particle volume

REFERENCES

- Brindley, G. W., 1951, X-ray Identification and Crystal Structures of Clay Minerals, The Mineralogical Society, London, 345 p.
- Jerlov, N. G., 1953, Influence of Suspended and Dissolved Matter on the Transparency of Sea Water, *Tellus*, 5:59-65.
- Jerlov, N. G., 1959, Maxima in the Vertical Distribution of Particles in the Sea, *Deep-Sea Research*, 5:173-184.
- Martin, B. D. and K. O. Emery, 1967, Geology of Monterey Canyon, *Amer. Assoc. Petrol. Geol. Bull.*, 5 (11):2281-2304.
- Mie, G., 1908, Beiträge zur optik trüber Medien speziell kolloidaler Metallösungen, *Ann. Physik*, 25:377.
- Morel, M. A., 1965, Interprétation des Variations de la Forme de l'Indicatrice de Diffusion de la Lumière par les Eaux de Mer, *Annales de Géophysique*, 21 (2):281-284.
- Paramonov, A. N., 1965, The Distribution Pattern of Suspended Matter in the Black Sea, *Oceanology*, 5(1):61-67.
- Sayles, F. L., 1966, A Reconnaissance Heavy Mineral Study of Monterey Bay Beach Sediments, University of California Hydrolic Engineering Laboratory, Tech. Report HEL 2-16, Berkeley, 20 p.
- Tyler, J. E., 1961, Scattering Properties of Distilled and Natural Water, *Limnol. Oceanog.*, 6:451-456.
- Wilde, P., 1965, Recent Sediments of the Monterey Deep-Sea Fan, University of California Hydrolic Engineering Laboratory, Tech. Report HEL 2-13, Berkeley, 153 p.
- Yancey, T. E., 1968, Recent Sediments of Monterey Bay California University of California Hydrolic Engineering Laboratory, Tech. Report HEL 2-18, Berkeley, 145 p.

INITIAL DISTRIBUTION LIST

	No. Copies
1. Defense Documentation Center Cameron Station Alexandria, Virginia 22314	2
2. Library, Code 0212 Naval Postgraduate School Monterey, California 93940	2
3. Department of Oceanography Naval Postgraduate School Monterey, California 93940	3
4. Commanding Officer and Director Naval Undersea Research & Development Center Attn: Code 2230 San Diego, California 92152	1
5. Director, Naval Research Laboratory Attn: Tech. Services Info. Officer Washington, D. C. 20390	1
6. Dr. Ned A. Ostenso Office of Naval Research Code 480 D Arlington, Virginia 22217	1
7. Oceanographer of the Navy The Madison Building 732 N. Washington Street Alexandria, Virginia 22314	1
8. Dr. Pat Wilde 438 Hearst Mining Bldg. University of California Berkeley, California	1
9. Naval Oceanographic Office Attn: Library Washington, D. C. 20390	1
10. National Oceanographic Data Center Washington, D. C. 20390	1

11. Director, Maury Center of Ocean Sciences 1
Naval Research Laboratory
Washington, D. C. 20390
12. Mr. Roswell W. Austin 1
Visibility Laboratory
Scripps Institution of Oceanography
La Jolla, California 92037
13. Dr. Wayne V. Burt 1
Department of Oceanography
Oregon State University
Corvallis, Oregon 97331
14. Dr. Peyton Cunningham 6
Department of Physics
Naval Postgraduate School
Monterey, California 93940
15. Dr. Siebert Q. Duntley 1
Visibility Laboratory
Scripps Institution of Oceanography
La Jolla, California 92037
16. Mr. George Eck 1
Naval Air Development Center
Johnsville, Warminster, Pennsylvania 18974
17. Mr. Gary Gilbert 1
Stanford Research Institute
Menlo Park, California 94025
18. Dr. R. C. Honey 1
Stanford Research Institute
Menlo Park, California 94025
19. Mr. Kenneth V. Mackenzie 1
Ocean Sciences Department - Code D503
Naval Undersea Research & Development Center
San Diego Division
San Diego, California 92152
20. Dr. Robert E. Morrison 1
AEL
Office of Environmental Systems
NOAA
6010 Executive Blvd.
Rockville, Maryland 20852
21. Mr. Jerry Norton 1
Oceanography Department
Naval Postgraduate School
Monterey, California 93940

22.	Mr. Larry Ott Naval Air Development Center Johnsville, Warminster, Pennsylvania 18974	2
23.	Mr. Thomas J. Shopple Naval Air Development Center Johnsville, Warminster, Pennsylvania 18974	1
24.	Mr. S. P. Tucker Department of Oceanography Naval Postgraduate School Monterey, California 93940	6
25.	Dr. Hasong Pak Department of Oceanography Oregon State University Corvallis, Oregon 97931	1
26.	Mr. Alan Baldridge, Librarian Hopkins Marine Station Pacific Grove, California 93950	1
27.	Mr. Ted Petzold Visibility Laboratory Scripps Institution of Oceanography La Jolla, California 92037	1
28.	Dr. Gary Griggs Division of Natural Sciences - II University of California, Santa Cruz Santa Cruz, California 95080	1
29.	Director Moss Landing Marine Laboratories Moss Landing, California 95039	1
30.	Mr. W. J. Stachnik Optical Systems U.S. Navy Underwater Sound Laboratory Fort Trumbull New London, Connecticut 06320	1
31.	LT M. Kazanowska The Madison Building 732 N. Washington St. Alexandria, Virginia 22314	1
32.	Mr. Raymond N. Vranicar Code AIR-370D Naval Air Systems Command Washington, D. C. 20360	2

33. Mr. Irvin H. Gatzke 2
Code AIR-370
Naval Air Systems Command
Washington, D. C. 20360
34. Dr. H. R. Gordon 1
Institute of Marine Sciences
University of Miami
10 Rickenbacher Causeway
Miami, Florida 33149
35. Dr. Robert Andrews 1
Department of Oceanography
Naval Postgraduate School
Monterey, California 93940
36. Mr. Robert Owen 1
Fishery-Oceanography Center
National Marine Fisheries Service
La Jolla, California 92037

DOCUMENT CONTROL DATA - R & D

(Security classification of title, body of abstract and indexing annotation must be entered when the overall report is classified)

1. ORIGINATING ACTIVITY (Corporate author) Naval Postgraduate School Monterey, California 93940		2a. REPORT SECURITY CLASSIFICATION Unclassified	
		2b. GROUP	
3. REPORT TITLE Suspended Matter in Monterey Bay, California: Some Aspects of its Distribution and Mineralogy			
4. DESCRIPTIVE NOTES (Type of report and, inclusive dates) Master's Thesis; September 1971			
5. AUTHOR(S) (First name, middle initial, last name) Maria Kazanowska			
6. REPORT DATE September 1971		7a. TOTAL NO. OF PAGES 84	7b. NO. OF REFS 11
8a. CONTRACT OR GRANT NO. b. PROJECT NO. c. d.		9a. ORIGINATOR'S REPORT NUMBER(S) 9b. OTHER REPORT NO(S) (Any other numbers that may be assigned this report)	
10. DISTRIBUTION STATEMENT Approved for public release; distribution unlimited.			
11. SUPPLEMENTARY NOTES		12. SPONSORING MILITARY ACTIVITY Naval Postgraduate School Monterey, California 93940	
13. ABSTRACT The distribution of suspended particulate matter in Monterey Bay, California, was characterized by the ratio of light scattering at 45° to that at 135°, by particle volume distributions, and by constituent distributions. X-ray methods were used to identify the mineral constituents. Distributions were highly variable with time and location. Although high scattering ratios and high volume distributions were found in the same vicinity, there appeared to be a lack of correlation between their absolute values. Scattering ratios were found to vary greatly with depth. The minerals detected in the water column at the Pajaro and the Salinas River mouths did not form separate and distinct regions. Of the characteristic minor constituents, jadeite was found to predominate in the Pajaro River area.			

KEY WORDS	LINK A		LINK B		LINK C	
	ROLE	WT	ROLE	WT	ROLE	WT
suspended matter						
suspended particulate matter						
particulate matter						
Monterey Bay suspended matter distribution						
mineralogy of suspended matter						
scattering ratio distribution in Monterey Bay						
light scattering						
X-ray scattering						
Coulter counter						

BINDERY

Thesis

132943

K1496 Kazanowska

c.1

Suspended matter in
Monterey Bay, California:
some aspects of
its distribution and
mineralogy.

BINDERY

Thesis

132943

K1496 Kazanowska

c.1

Suspended matter in
Monterey Bay, California:
some aspects of
its distribution and
mineralogy.

thesK1496

Suspended matter in Monterey Bay, Califo



3 2768 002 11168 4

DUDLEY KNOX LIBRARY